SMALL-SIGNAL STABILITY ASSESSMENT USING A DYNAMIC PHASOR APPROACH: A CASE STUDY OF A 2MVA WIND POWER PLANT

Kaha Widanalage Don Chalitha Kanchana
(149308K)

Thesis/Dissertation submitted in partial fulfilment of the requirements for the degree Master of Science in Electrical Installation

Department of Electrical Engineering

University of Moratuwa
Sri Lanka

March 2019

DECLARATION

I declare that this is my own work and this thesis does not incorporate without acknowledgement any material previously submitted for a Degree or Diploma in any other University or institute of higher learning and to the best of my knowledge and belief it does not contain any material previously published or written by another person except where the acknowledgement is made in the text.

Also, I hereby grant to University of Moratuwa the non-exclusive right to reproduce and distribute my thesis, in whole or in part in print, electronic or other medium. I retain the right to use this content in whole or part in future works (such as articles or books).

Signature: Date:

The above candidate has carried out research for the Master thesis under my supervision.

Signature of the supervisor:

Dr. W. D. Prasad Date:

DEDICATION

This work is dedicated to my beloved parents, Mr: Samarapala Kahawidane and Mrs: Chandra Piyawathi.

ACKNOWLEDGMENT

I would like to sincerely thank my internal supervisor, Dr. W.D. Prasad (Department of Electrical Engineering, University of Moratuwa) for the continuous support provided throughout my research. If that guidance, encouragement and expertise knowledge in the theoretical side is not there, I would not be able to finish my work in time.

My batch mate Eng. Roshan Akarawita (Windforce.Pvt.Ltd) helped me a lot by providing data on wind power plants in Puttalam area and providing details on Sri Lankan wind power generation. I would also like to thank him for the support that he has given, even with his busy schedule.

For my simulation work and calculations, computer laboratory of Electrical Engineering Department, University of Moratuwa helped me providing PSCAD and MATLAB software access. Also for the literature analysis I got the access to the IEEE library through the computer laboratory. I would be grateful for the support made by the friendlier staff by letting me the access to the laboratory whenever necessary.

Last but not least I would like to offer my sincere gratitude to my parents who had backed me and encouraged me throw-out the research period.

Abstract

Due to the technical development, support from the green energy enthusiasts and relative cost attractiveness wind energy harvesting has turn into one of the most popular renewable energy sources nowadays. When considered together with wind power plants, other power plants and transmission lines; power system has become a dynamic system which includes non-linear elements. Evaluating non-linear system with linearized method may not be sufficient to evaluate the system. Hence, advanced linear mathematical model is needed to study the wind plants connected to the grid and its oscillations. In this research, a linearized model developed with dynamic phasor approach combined with conventional small signal stability analysis is presented to analyze wind power system. The model developed is compatible with type 4 wind power plants in any capacity and can be adopted in any power system where system specifications are known.

With the help of 2MVA test system; model validation, stability analysis and a sensitivity analysis using participation factors will be carried out in order to identify dominant oscillations introduced to the grid from the plant.

Keywords: wind turbines, small signal stability analysis, dynamic phasors, linearized model, model validation, sensitivity analysis, participation factors

Table of Contents

DECLARATION I
DEDICATION II
ACKNOWLEDGMENT III
Abstract IV
Table of Contents V
List of Figures VII
List of Tables VII
List of Abbreviations VIII
1 INTRODUCTION 1
1.1 Wind power 1
1.1.1 Sri Lanka wind power generation 3
1.1.2 Different types of Wind Turbine-Generators 4
1.2 Power system stability 7
1.2.1 Power system stability/Sub-synchronous Interaction Analysis Techniques 7
1.2.2 Dynamic Phasors 10
1.3 Objectives of the study 12
1.4 Thesis outline 12
2 Modelling of a wind power plant 14
2.1 Wind turbine model 15
2.2 Drive train model 17
2.3 Permanent Magnet Synchronous Generator (PMSG) model 19
2.4 Generator Side Converter (GSC) model 21
2.5 DC connecting link model 23
2.6 Voltage Source Inverter (VSI) model 24
2.7 Transmission cable model 26
2.8 Final model 27
3 RESULTS AND ANALYSIS 30
3.1 Model stability 30
3.2 Model validation using PSCAD 33

3.3 Sensitivity analysis 34
4 CONCLUSIONS AND FUTURE DIRECTIONS 37
4.1 Conclusions 37
4.2 Future Directions 38
5 REFERENCES 39
6 Appendix 42
6.1 Appendix A – test system values 42
6.2 Appendix B – Final wind plant model 43

List of Figures

Page

Figure 1 - Growth of world wind energy generation 1
Figure 2- Countries which generate highest wind energy 2
Figure 3 – Wind power density in Sri Lanka 3
Figure 4 - Renewable energy growth estimation 4
Figure 5 - Different types of wind turbine generators..... 6
Figure 6 - Power system transients 10
Figure 7 - Typical components of a type4 wind turbine 14
Figure 8 - λ VS C_p variation at constant β values 16
Figure 9 - Turbine speed VS power variation at constant wind speeds 16
Figure 10 - Turbine mechanical dynamics..... 18
Figure 11 - Generator d-q axis representation 19
Figure 12- Equivalent circuits for d-and q axises 20
Figure 13 - Generator side converter representation..... 22
Figure 14 - DC link representation..... 23
Figure 15 - Voltage source inverter model representation..... 24
Figure 16 - Representation of transmission line 26
Figure 17 - Inputs/outputs of blocks which creates the wind plant..... 27
Figure 18 - Summary of state variables 28
Figure 19 - Generator speed after small disturbance 32
Figure 20 - PSCAD simulation model 33
Figure 21 - Generator speed variation..... 34
Figure 22 - Wind speed variation..... 34
Figure 23 - Future scope 38

List of Tables

Page

Table 1 - Eigenvalues of the 2MVA test system..... 32
Table 2 - Partcipation factors 35

List of Abbreviations

Abbreviation	Description
NE	North East
SW	South West
CEB	Ceylon Electricity Board
NREL	National Renewable Energy Laboratory
SEA	Sustainable Energy Authority
ADB	Asian Development Bank
DFIG	Doubly-Fed Induction Generators
SSI	Sub-Synchronous Interaction
VSC	Voltage Source Converter
PMSG	Permanent Magnet Synchronous Generator
GSC	Generator Side Converter
VSI	Voltage Source Inverter
TSR	Tip Speed Ratio
PWM	Pulse-Width Modulation
MPPT	Maximum Power Point Tracking
IGBT	Insulated-Gate Bipolar Transistor

1 INTRODUCTION

1.1 Wind power

For many years, demand for electricity was provided by fast diminishing traditional energy sources like hydro, nuclear and fossil fuels. It took years to understand that electricity generation from fossil fuels and nuclear energy comes with a price for the environment as well as living beings. Therefore at present, many countries have made their plans to cater the electricity demand of the country from alternative energy sources. As the technology became more and more advanced, support from the green energy enthusiasts and relative cost attractiveness wind energy harvesting has turn into one of the most popular renewable energy sources nowadays. [**1**]

As per the preliminary statistics report published by World Wind Energy Association, all together 539,291 MW capacity of wind turbines were installed worldwide by the end of 2017. As per the report 52,552 MW were added to the global energy generation in the year 2017, a little more capacity than in 2016 (51,402 MW). It is said that 5% of global electricity demand is covered by the generated capacity of wind turbines added to the grid at the end of year 2017. All over the globe, wind power generation has turn out to be the key factor in their power generation strategies to eliminate fossil and nuclear energy generation. In 2017, Denmark has made a new world record of generating 43% of its energy demand from wind power harvesting. Today number of countries all over the world had increased their wind power generation beyond 10% bench mark, including Germany, Portugal, Ireland, Sweeden and Uruguay. [**2**]

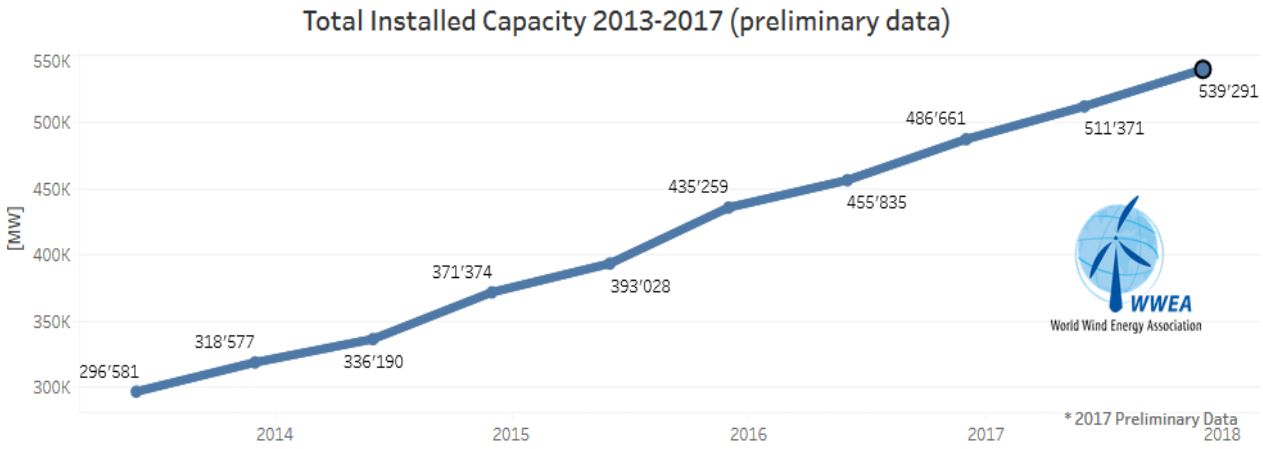

Figure 1 - Growth of world wind energy generation [**2**]

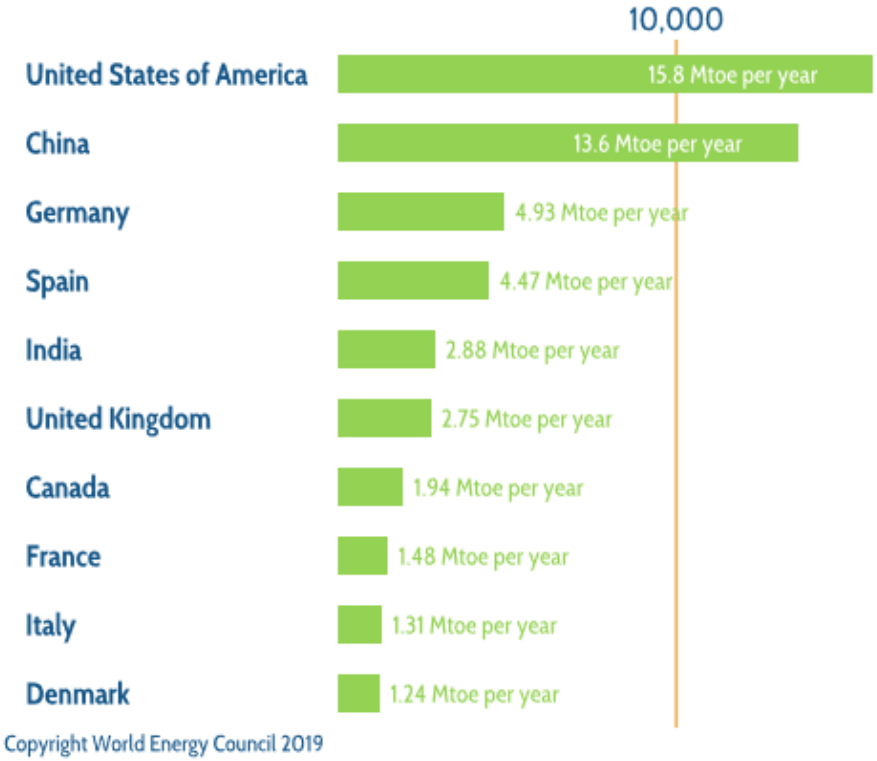

Figure 2- Countries which generate highest wind energy [**2**]

The main disadvantage of wind power is its fluctuation and randomness. As the wind became unpredicted and intermittent, the power generation becomes the same and causes a great impact on the power system stability. Engineers & scientists have given intensive attention to this issue and wind farm arrangement and equipment are in a continuous development process.

1.1.1 Sri Lanka wind power generation

Sri Lanka's wind climate is based on two main Asian Monsoons namely the South West monsoon (SW) and North East (NE) monsoon. The SW Monsoon is starting from May and will be there until early of October. The NE Monsoon is starting from December and will be there until February. The SW monsoon is said to be the heaviest among two and it provides rain for entire West Coast together with some mountainous regions inside of Sri Lanka.

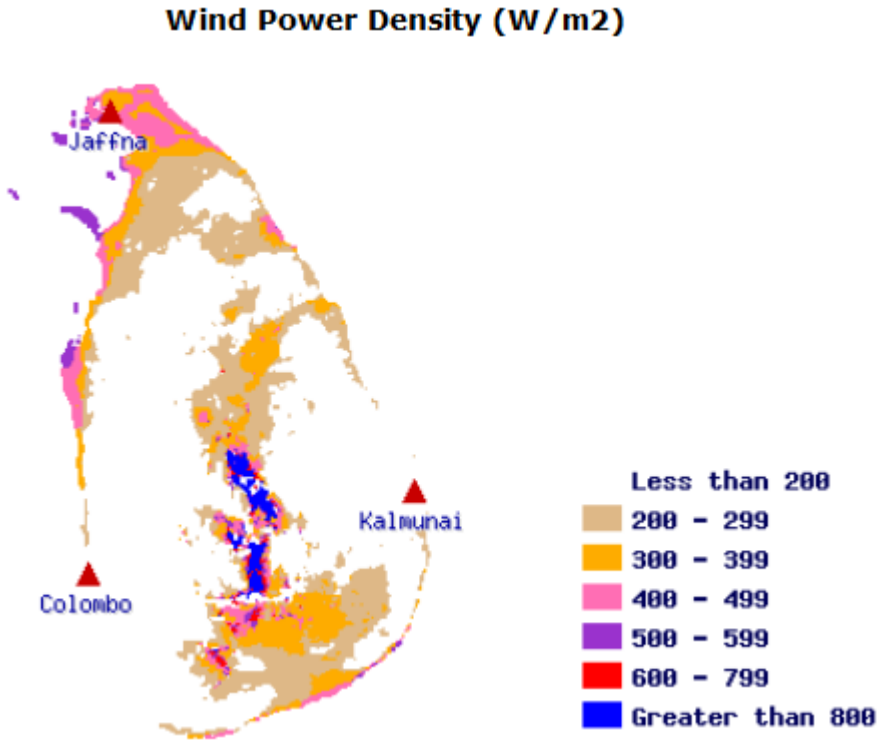

Figure 3 – Wind power density in Sri Lanka [**3**]

Initial wind studies were being performed by Ceylon Electricity Board (CEB) in early 2000/2002 based on some selected areas throughout country by put in wind masts. After that, The National Renewable Energy Laboratory (NREL) of USA performed a full study using satellite mapping technique not only for Sri Lanka, but also for Maldives. The results came revealing that Sri Lanka got a wind power potential of 20,740 MWs. After forming the institute of Sustainable Energy Authority (SEA) in 2007, several more researches were performed throughout the country installing wind masts at several locations. [**4**]

The first step of wind power plants was taken in 1999 by installing 3MW turbine closed to Hambantota by the CEB. Although the project was a failure, it gave a good start. After year 2016 contribution from wind power was 128.4 MW. It was such a way that; 128.4MW out of 516 MW of other renewable energy plants that were

commissioned. It consists of 15 number of wind power plants where maximum of one plant is limited to 10 MW. It has been identified Mannar area situated in the Northern Province as the best location for installing mass no of wind poer plants forming a wind farm. Not limiting to that, CEB has already started to make the first 100MW wind farm in above mentioned Mannar Island with the help of of Asian Development Bank (ADB). It was calculated that 100MW project will produce 320 GWh of energy throughout the year for the national increasing energy demand. Required infrastructure and basic requirements will be also developed in the southerncoast of Mannar island, which is the selected place for first plant. [**5**]

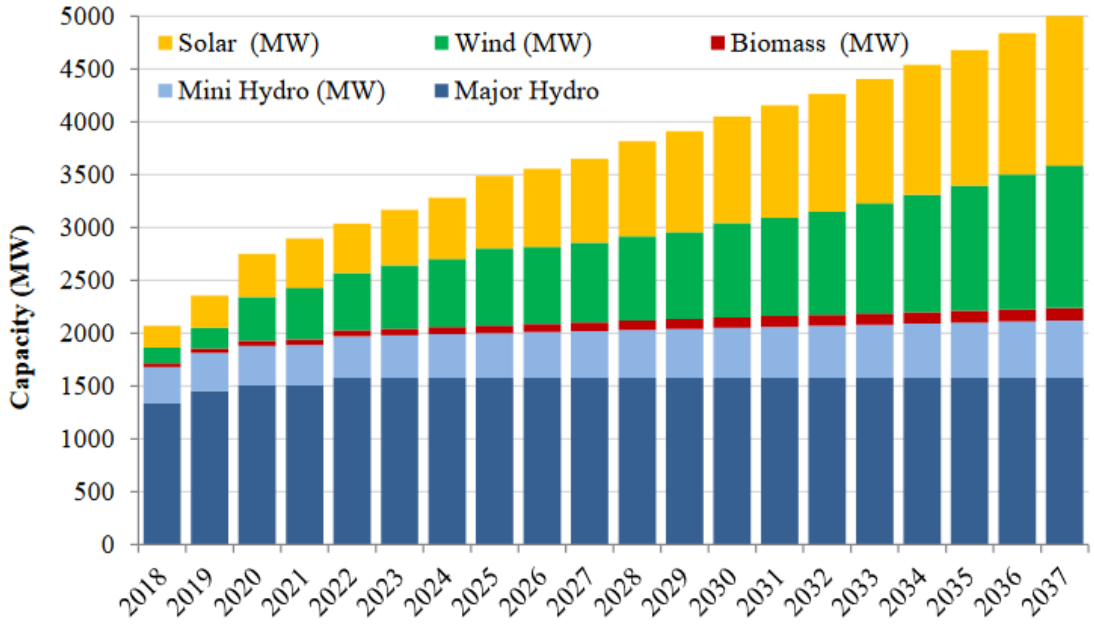

Figure 4 - Renewable energy growth estimation [**5**]

1.1.2 Different types of Wind Turbine-Generators

Considering the operational arrangement, wind turbine generator assembly can be categorized as fixed-speed type or variable-speed type wind turbine-generators. In the fixed speed type the generator could be either a squirrel cage or a wound rotor type one. It is directly linked to the grid network with the support of a soft starting method and a capacitor bank. In this arrangement of wind turbine-generator, the unit is designed to operate optimally only for one rotor speed. As the generator is directly connected to the power grid network, the torque fluctuations occurred due to the wind speed fluctuations are transmitted to the grid ac network as power transients. Although the capacitor provides reactive power support, the reactive power consumption of a fixed-speed wind turbine cannot be controlled.

The main advantages of this type of wind turbine-generators are that they are simple, robust and inexpensive.

Unlike the fixed speed type, the variable-speed type wind turbines designed to operate in a range of speeds, optimal manner. Also, the reactive power consumption can be controlled by means of the power electronic converter present in most variable speed type wind turbine/generator arrangement. Although, controlling of variable-speed wind turbine/generator arrangement is complex and they are expensive when compared to the fixed-speed wind turbine-generators.

Type 1 wind turbine generators

- Fixed-speed wind turbine-generator as it does not support varying the turbine speed.
- Use wound rotor induction generators.
- Capacitor bank arrangement is used to limit reactive power consumption from the AC network.

Type 2 wind turbine generators

- Almost identical to the type 1.
- A limited speed control can be achieved by using the variable rotor resistor. The range of speed controlling changes with size of the external rotor resistor. Normally a speed margin of 0-10% beyond the synchronous speed can be achieved. [**1**]

Type 3 wind turbine generators

- Use wound rotor induction generators.
- The generator is linked to the power grid network through a partially rated converter. The converter needs to be rated at only 1/3 of the rating of the generator. [**3**]
- Another calling name is Doubly-Fed Induction Generators (DFIG).
- Because of the additional controllability provided by the converter, the reactive power consumption/supply with the power grid network can be controlled precisely.
- The dynamic speed rage of the Type 3 wind turbine-generators vary with the capacity of the converter and normally a speed range of 70% to 130% of the synchronous speed is possible.

Type 4 wind turbine generators

- These are connected to the AC network via a fully rated converter.
- Since the converter de-couples the wind turbine from the ac network, the machine is able to run at any speed.

- The reactive power supply/consumption with the grid network can be precisely controlled similar to the type 3 units.
- Type 4 wind plants are expensive compared to Type 3 wind turbine-generators as they use fully rated converters.

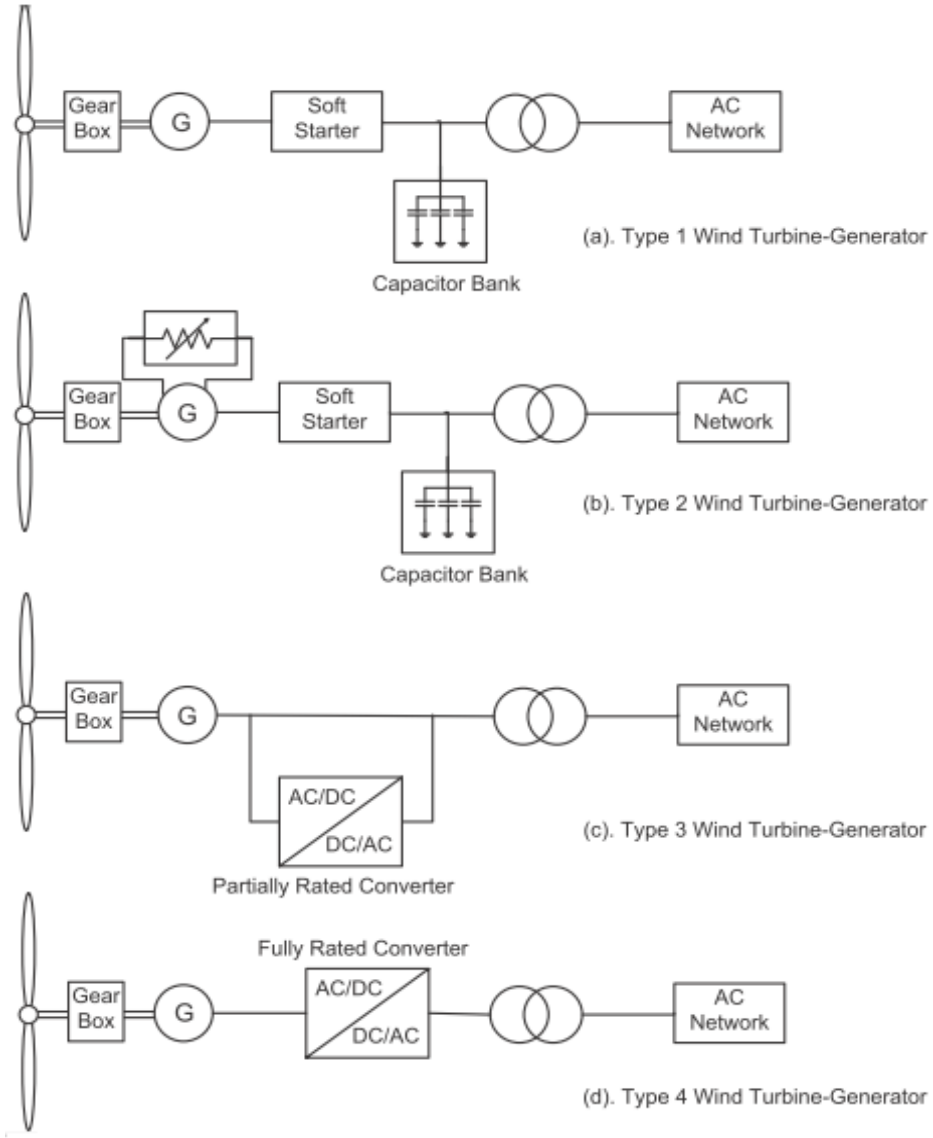

Figure 5 - Different types of wind turbine generators

Because of their reactive power controllability, Type 4 wind turbine-generators are widely used nowadays. Hence the work presented in this thesis is focused on Type 4 wind turbine-generators.

1.2 Power system stability

By using the term “power system stability”, we mean the ability to maintain synchronism (ability to remain in equilibrium under normal condition or come back to an acceptable level of equilibrium) when subjected to a disturbance. This can be caused by a transient disturbance of wind power variation, transmission line fault, loss of a load….etc. [**7**] Normally synchronous machines are the main electrical power generators of the power system. So the main condition for a satisfactory system is that all synchronous machines have to be in synchronism. As we go through this point it is clearly understandable that stability is highly depend on dynamics of gen. rotor angles and power-angle relationship. Next thing is the way of evaluating the stability; the idea or the expectation is to study the behaviour/movement of the power system when it faces to a transient disturbance. The disturbance can be a small-one or large-one. Small disturbances; produced by the system load changes can occur continually. But the system changes the parameters by itself to adjust the changing conditions.

A power system is a large combination of electrical and mechanical elements. The electrical system has many series and parallel combinations of inductive, capacitive, and resistive elements. Each series and parallel combination has a natural frequency. Therefore, the electrical system has many natural frequencies and typically they are well above the system operating frequency, which is either 60 or 50Hz.Often these higher frequency oscillations are well damped. Even if an under-damped oscillation is present, it can be easily filtered out. However, under certain conditions such as in the presence of series compensation, some of these natural frequencies can be below the nominal operating frequency. In such cases, they can interfere with the normal operation of the power system. [**8**]

1.2.1 Power system stability/Sub-synchronous Interaction Analysis Techniques

Several techniques are available to study or analyse sub-synchronous interactions (SSI) & power system stability in power systems. The main objective of these techniques is to identify the potential conditions and locations that can create sub-synchronous interactions in various power system components. Once they are identified, the power system can be designed either to avoid such conditions, or to protect it from reaching undesirable operating conditions such as excessive voltages and currents. Also, these techniques will aid the design of appropriate mitigation measures.

Following are some analysis techniques that are presently being used.

1.2.1.1 Small signal stability analysis

The small signal stability analysis carried out on a dynamic system gives insight into the oscillatory behaviour of the system. The eigenvalues calculated from the linearized equations of the nonlinear system are used for the small signal analysis. Analysis of the eigenvalues reveals the damping frequency and the number of oscillatory modes present in the system. Also, the Eigen structure information derived from the linearized system is used to obtain the participation factors and mode shapes, which are used to identify the root cause of the oscillations. [**9**], [**10**], [**11**], [**12**]

However, small signal analysis is not meant for time domain simulations as linearized models are only valid for small disturbances in the system.

Linearized power system model approach [**7**]

The dynamic behaviour of a power system can be shown using a set of non-linear differential equation as mentioned below. There ***n*** represents the order of the system and ***r*** represents the number of inputs.

$$\dot{x}_i = f_i(x_1, x_2, ..., x_n; u_1, u_2, ..., u_r; t) \qquad i = 1,2,....,n \tag{1.1}$$

This can be re-written in vector-matrix notation as below.

$$\dot{x} = f(x,u) \tag{1.2}$$

Where;

$$x = \begin{bmatrix} x_1 & x_2 & \dots & x_n \end{bmatrix}^T; \qquad u = \begin{bmatrix} u_1 & u_2 & \dots & u_r \end{bmatrix}^T; \qquad f = \begin{bmatrix} f_1 & f_2 & \dots & f_n \end{bmatrix}^T$$

Here ***x*** is called the state vector and ***u*** is called the input vector. As ***f*** is independent of time these systems are called invariant systems or autonomous systems. To be linearized, the system should be autonomous. As a power system for a given system configuration and for a given condition can be expressed in equation 1.2 form, it is considered as an autonomous system.

When non-linear system is linearized, an equilibrium point is defined and Taylor series expansion is used neglecting second & higher order powers. At this equilibrium point, derivatives of states are zero.

$$\dot{x}_0 = f(x_0, u_0) = 0 \tag{1.3}$$

For a small perturbation around steady state point, the states and inputs become;

$$x = x_0 + \Delta x \qquad u = u_0 + \Delta u \tag{1.4}$$

Then equation 1.2 can be written as below.

$$\dot{x} = \dot{x}_0 + \Delta\dot{x} = f[(x_0 + \Delta x),(u_0 + \Delta u)] \tag{1.5}$$

Using Taylor series expansion, neglecting second and higher order terms;

$$\dot{x}_i = \dot{x}_{i0} + \Delta\dot{x}_i = f_i(x_0,u_0) + \frac{\partial f_i}{\partial x_1}\Delta x_1 + ...+ \frac{\partial f_i}{\partial x_n}\Delta x_n + \frac{\partial f_i}{\partial u_1}\Delta u_1 + ...+ \frac{\partial f_i}{\partial u_r}\Delta u_r \tag{1.6}$$

Since $\dot{x}_{i0} = f(x_0,u_0)$ we obtain,

$$\Delta\dot{x}_i = \frac{\partial f_i}{\partial x_1}\Delta x_1 + ...+ \frac{\partial f_i}{\partial x_n}\Delta x_n + \frac{\partial f_i}{\partial u_1}\Delta u_1 + ...+ \frac{\partial f_i}{\partial u_r}\Delta u_r \tag{1.7}$$

This equation 1.7 can be represented as in below equation;

$$\dot{x} = A\Delta x + B\Delta u \tag{1.8}$$

Here ***A*** is known as the state or plant matrix and ***B*** is known as the control or input matrix.

1.2.1.2 Frequency scanning

In frequency scanning, the presence of a network resonance is identified by calculating the driving point impedance over the entire sub-synchronous frequency spectrum. A sharp change in the impedance indicates a network resonance. The complementary frequency of the network resonance gives the resulting sub-synchronous interaction frequency. This is a widely used method to study and identify sub-synchronous interactions developed in power systems with thermal generation. Frequency scanning is mainly used as a screening technique. [**13**]

1.2.1.3 Electromagnetic transient simulations

Electromagnetic transient simulation uses detailed models that take into account the non-linear characteristics of power system components. [**14**] Therefore it gives the closest results to the actual behaviour of the power system. Hence, electromagnetic transient simulation has been used to study and identify sub-synchronous interactions developed in power systems. [**9**], [**10**] Dynamic behaviour of the system even under large system disturbances such as faults can be accurately studied using electromagnetic transient simulations.

1.2.1.4 Damping torque analysis

Damping torque analysis is mainly used to identify the potential sub-synchronous torsional interaction problems. [**15**] This method is mainly used when the mechanical shaft data are not readily available and the torsional oscillation frequencies are known. In this method, a small sinusoidal perturbation was added to the machine's speed reference and the corresponding change in electrical torque in phase with the speed is measured. This is used to estimate the inherent damping added by the electrical system at a particular torsional frequency. When performing the damping torque analysis the mechanical system needs to be decoupled from the electrical system.

1.2.2 Dynamic Phasors

Phasor-analysis involves representing sinusoidal quantities as complex numbers using only their magnitude and phase, in steady state. Standard phasors-analysis is used in conventional electromechanical transient simulators to represent the electrical network.

Following is block diagram which indicates the differences between Electromechanical and Electromagnetic transient analysis. Conventional small signal stability analysis falls in to the electromechanical transient analysis category. Transient analysis carried out using sophisticated software like PSCAD, PSSE falls in to the electromagnetic transient analysis category. As we use dynamic phasors together with conventional small signal stability analysis it falls somewhere between electromechanical and electromagnetic transient analysis, which means more effective in studies.

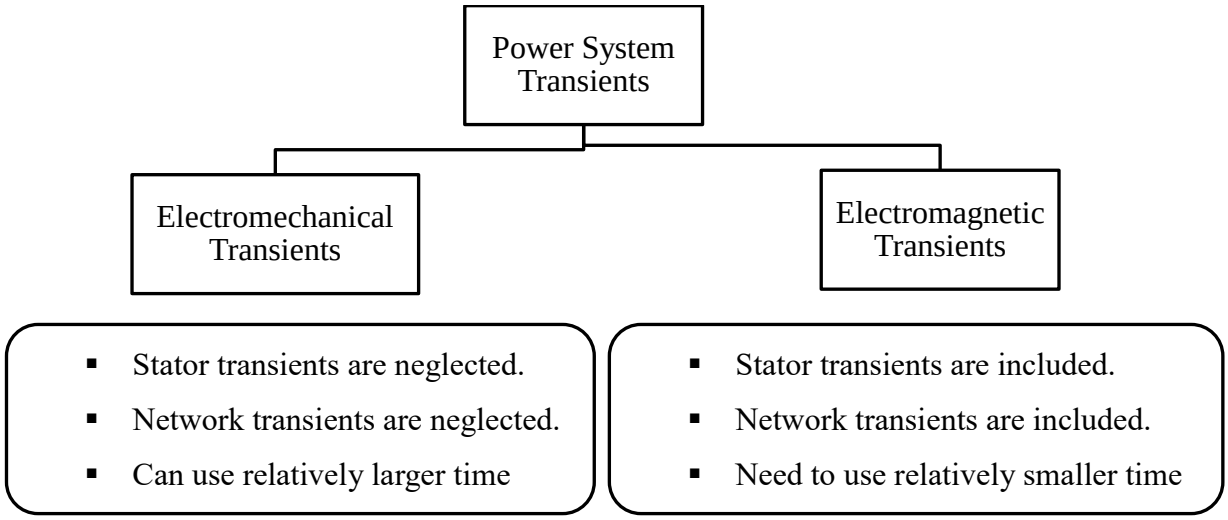

Figure 6 - Power system transients

The basic building blocks of the dynamic phasor ac network model are the series RL circuit and the parallel RC circuit. The aforementioned passive network elements can be synthesized into series combinations of RL components and parallel combinations of RC components. Then each synthesized component can be easily represented using dynamic phasors as follows.

Series R-L circuit [**16**]

Consider a series R-L component linked between nodes 1 and 2. Then the instantaneous voltage between those nodes can be represented as below.

$$V_{12} = L\frac{di_{12}}{dt} + Ri_{12} \tag{1.9}$$

The complex phasors relationship of the currents and voltages can be substituted to the equation 1.9 as follows.

$$(V_R + jV_I)e^{jw_0t} = L\frac{d\{(i_R + ji_I)e^{jw_0t}\}}{dt} + R(i_R + ji_I)e^{jw_0t} \tag{1.10}$$

By assuming nominal frequency (ω_0) is constant following equation can be obtained.

$$(V_R + jV_I) = L\frac{d(i_R + ji_I)}{dt} + (R + jw_0L)(i_R + ji_I) \tag{1.11}$$

Parallel R-C circuit [**16**]

Consider a parallel R-C circuit linked between node 1 and the ground. The instantaneous currents injected to the circuit can be written as below.

$$i = C\frac{dV_1}{dt} + \frac{1}{R}V_1 \tag{1.12}$$

The complex phasors relationship of the currents and voltages can be substituted to the equation 1.12 as follows.

$$(i_R + ji_I)e^{jw_0t} = C\frac{d\{(V_{1R} + jV_{1I})e^{jw_0t}\}}{dt} + \frac{1}{R}(V_{1R} + jV_{1I})e^{jw_0t} \tag{1.13}$$

The phasor relationship similar to 1.11 is given by;

$$(i_R + ji_I) = C\frac{d(V_{1R} + jV_{1I})}{dt} + (\frac{1}{R} + jw_0C)(V_{1R} + jV_{1I}) \tag{1.14}$$

1.3 Objectives of the study

Power system is a dynamic system which includes non-linear elements. Evaluating non-linear system with linearized method may not be sufficient to evaluate the system. Hence, advanced linear mathematical model is needed to study the wind plants connected to the grid and its oscillations.

The main objective is to develop a mathematical model by identifying the required blocks for modeling. This mathematical model can be used to analyze a wind power plant/farm connected to Sri Lankan power system, if specifications of the plant are known.

2 MVA wind plant was selected as a test system to validate the developed model and sensitivity analysis was carried out to identify & investigate the dominant oscillations produced by the test system.

The key objectives made to achieve the goal are:

- Identifying the required blocks for modeling.
- Developing the small-signal stability model of the wind power plant and validate the model.
- Identifying the dominant oscillations introduced by the wind plant into the system.

1.4 Thesis outline

In order to achieve the objectives mentioned in Section 0 above, the rest of the thesis is organized as follows:

Chapter 1 presents introduction, literature review on the wind power generation and power system stability analysis.

Chapter 2 presents the methodology carried out to develop the advanced linear mathematical model.

Chapter 3 presents the validation of the developed mathematical model and sensitivity analysis results based on 2 MVA test system.

Chapter 4 presents the conclusions and future directions of the study.

Chapter Summary

The present chapter (Chapter 1) gives an introduction about wind power generation and wind power plants together with a literature review of available power system stability analysis methods.

Next chapter will discuss the methodology adapted in modelling, simplifying and linearizing the main components identified in wind power plant and forming the complete model of a wind power system/plant.

2 Modelling of a wind power plant

A commonly used type-4 wind turbine generator arrangement is displayed below.

A wind turbine is attached to a permanent magnet synchronous generator together with a gear box. Gear box is used to match wind turbine speed with the generator synchronous speed as wind turbine rotates at a lower speed. Generator output is coupled to a fully rated converter called Generator Side Converter (GSC). Converter output is DC voltage and smoothing capacitor is provided in this DC link to reduce the repelling effect. At the end of DC link there is an inverter which converts DC into line voltage. A step-up transformer is used to step up the voltage in to distribution voltage and plant is connected to the nearest grid-substation through a transmission line (a shielded cable).

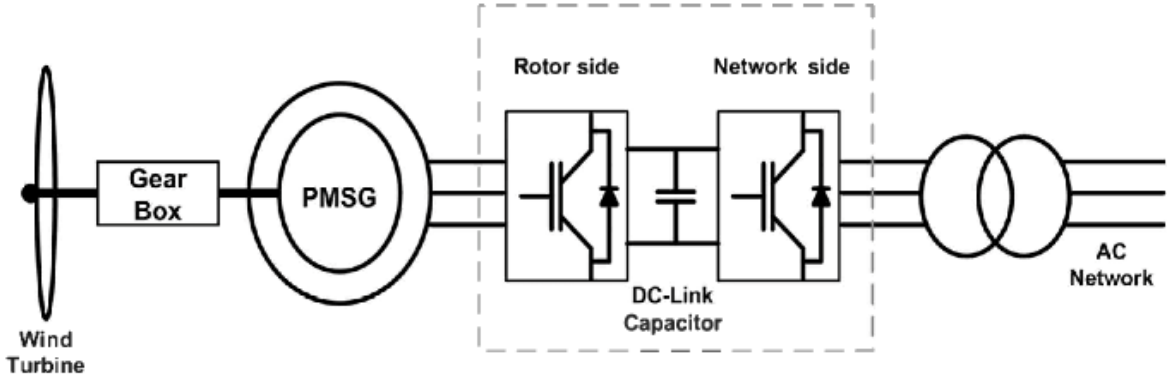

Figure 7 - Typical components of a type4 wind turbine

After studying previous works/researches on this field, following blocks were identified as main components of the wind power plant which are needed to be modelled to analyse the stability. (Here in this research, wind power plant is considered as connected to an infinite bus)

1. Wind turbine
2. Drive train
3. Permanent Magnet Synchronous Generator (PMSG)
4. Generator Side Converter (GSC)
5. DC link
6. Voltage Source Inverter (VSI)
7. Transformer and transmission line

Rest of the chapter describes the methodology followed to model each block, create linearized equation for the block and combining all blocks together to make the complete linearized model of the wind power plant.

2.1 Wind turbine model

The mathematical equation for wind power extraction by a wind turbine is given by,

$$P_W = 0.5\pi\rho R^2 C_P V_w^3 \tag{2.1}$$

ρ = air density in [kg/m^3]
R = turbine blade length in [m]
C_P = performance coeficient
V_W = wind speed perpendicular to turbine in [m/s]

The performance coefficient is a function of Tip Speed Ratio(TSR)-λ, and pitch angle-β. The maximum theoretical value of the performance coefficient is 59.3%. This value is known as the Betz limit. But in the commercial turbines in the field performance coefficient - C_p varies 20%-45%. [**9**] Tip speed ratio is defined as,

$$\text{Tip speed ratio } (\lambda) = \frac{\text{turbine blade tip speed}}{\text{wind speed}} = \frac{\omega_r R}{V_W} \tag{2.2}$$

As per the previous researches done on wind turbines, we can represent C_p as below. [**10**]

$$C_p(\lambda,\beta) = C_1\left(\frac{C_2}{\alpha} - C_3\beta - C_4\right)e^{\left(\frac{-C_5}{\alpha}\right)+C_6\lambda} \tag{2.3}$$

$$with\ \frac{1}{\alpha} = \frac{1}{\lambda + 0.08\beta} - \frac{0.035}{\beta^3 + 1}$$

The coefficients c_1 to c_6 are: c_1=0:5176, c_2=116, c_3=0:4, c_4=5, c_5=21 and c_6=0.0068. If we model the variation of C_p with reference to the λ, at a constant β, the graph will look like below. [**8**]

As shown in below graph, each pitch angle has an optimum value of λ where Cp gets maximum. From turbine power equation we can see that if the wind turbine is operated at this optimum Cp, the power extracted from the wind is maximum for a given wind speed. Therefore, often wind turbines are operated at this optimum tip speed ratio. This operating mode is commonly referred to as maximum power tracking mode. [**7**]

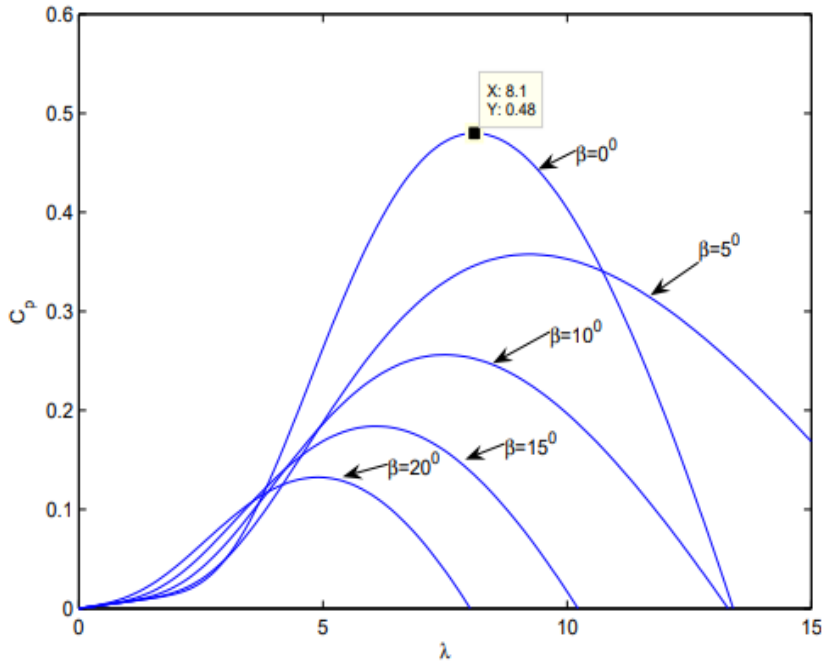

Figure 8 - λ VS C_p variation at constant β values

A typical wind turbine characteristic where turbine power variance with reference to the generator shaft speed (turbine rotation speed) is shown below. [**8**] There, as the wind speed changes, the generator speed (turbine rotation speed) is changed by the speed controller in order to keep the λ at its optimum-value.

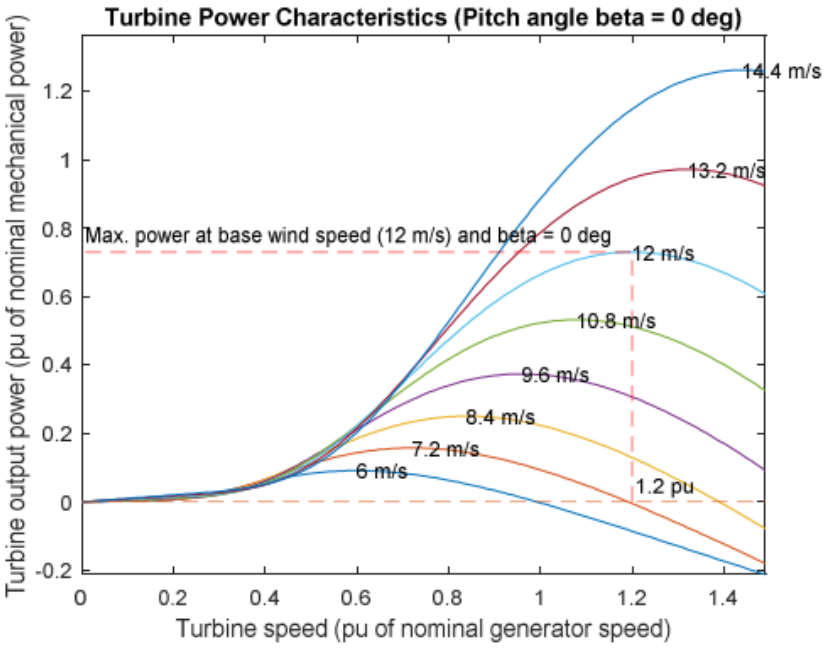

Figure 9 - Turbine speed VS power variation at constant wind speeds

The wind speed where the turbine extracts its rated power is called the rated wind speed. If the wind speed increases beyond the rated speed, the machine is forced out of the optimal TSR operation. In such a case the pitch controller changes the pitch angle of the turbine blades (β) so that the power extracted by the wind turbine is limited to the rated power. Otherwise, it is kept constant at $\beta = 0^{\circ}$.

Here in this research only operating conditions under the rated wind speed will be considered, hence, it does not influence the small-signal modelling. Turbine power (P_w) or Turbine torque (T_w) will be considered as an input to the overall system.

$$P_W = 0.5\pi\rho R^2 C_P V_w^3 \tag{2.4}$$

$$T_W = \frac{P_W}{\omega} = \frac{0.5\pi\rho R^2 C_P V_w^3}{\omega} \tag{2.5}$$

Here ω is the rotational speed of the turbine.

2.2 Drive train model

The drive train model represents wind farm's main mechanical dynamics. Several models of varying degrees of complexity were used in previous researches for drive train modelling. One-mass [**7**], [**11**], [**12**], two-mass [**13**], [**14**], [**15**] and three-mass [**16**], [**17**], [**18**] are the most common models among them.

In one-mass model generator inertia, turbine hub and blades are considered as a single lumped mass. In two-mass model, wind turbine and the generator are modelled as two masses connected via a flexible shaft. In three-mass model the flexible portion of the blade is considered as one mass, the rigid part of the blades and turbine hub as another mass and the generator as the third mass. Although simple, one-mass model is not capable of showing torsional oscillations in the wind power plant. The two-mass model is capable of showing torsional oscillation between the wind turbine and the generator at an observable limit. When the complex machine dynamic studies are needed, the three-mass model can be adopted. When consider a problem where torsional fatigues are needed to be studied, dynamics related to all parts of turbine-generator arrangement have to be analysed. Hence for this study two-mass model is used as it is sufficient enough to study system mechanical dynamics.

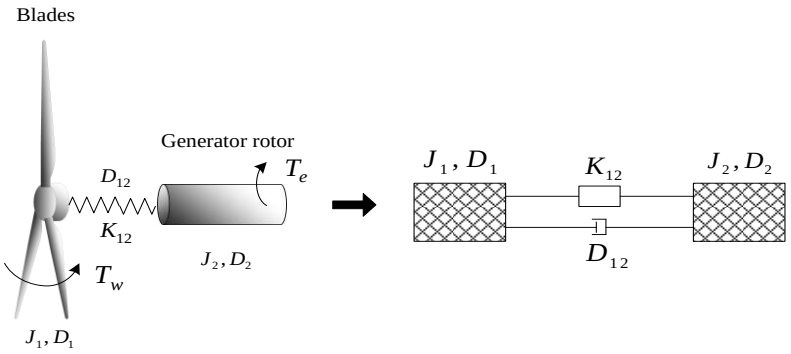

Figure 10 - Turbine mechanical dynamics

Using Hooke's law and Newton second law, the two-mass model of the shaft of a generator- wind turbine arrangement can be analysed by the dynamic equations mentioned below.

$$\Delta\dot{\theta}_1 = \Delta\omega_1 \tag{2.6}$$

$$\Delta\dot{\theta}_2 = \Delta\omega_2 \tag{2.7}$$

$$J_1\Delta\dot{\omega}_1 = \Delta T_W - D_1\Delta\omega_1 - D_{12}(\Delta\omega_1 - \Delta\omega_2) - K_{12}(\Delta\theta_1 - \Delta\theta_2) \tag{2.8}$$

$$J_2\Delta\dot{\omega}_2 = \Delta T_e - D_2\Delta\omega_2 - D_{12}(\Delta\omega_2 - \Delta\omega_1) - K_{12}(\Delta\theta_2 - \Delta\theta_1) \tag{2.9}$$

Where,
T_w – aero-dynamic torque produced from the turbine
T_e – electro-mechanical torque produced from the generator
J_1 & J_2 – moment-of-inertia of blades, generator shaft/rotor
D_1 & D_2 - damping factor of blades, generator shaft/rotor
K_{12} - stiffness coefficient of blades, generator shaft/rotor
D_{12} - damping coefficient of blades, generator shaft/rotor

By linearizing the above equations, we can form the block in following form.

$$\Delta\dot{\boldsymbol{X}}_M = \boldsymbol{A}_M\Delta\boldsymbol{X}_M + \boldsymbol{B}_M\Delta\boldsymbol{u}_M \tag{2.10}$$

$$\begin{bmatrix} \Delta\dot{\theta}_1 \\ \Delta\dot{\theta}_2 \\ \Delta\dot{\omega}_1 \\ \Delta\dot{\omega}_2 \end{bmatrix} = \begin{bmatrix} 0 & 0 & 1 & 0 \\ 0 & 0 & 0 & 1 \\ -\frac{K_{12}}{J_1} & \frac{K_{12}}{J_1} & -\frac{D_1 + D_{12}}{J_1} & \frac{D_{12}}{J_1} \\ \frac{K_{12}}{J_2} & -\frac{K_{12}}{J_2} & \frac{D_{12}}{J_2} & -\frac{D_2 + D_{12}}{J_2} \end{bmatrix} \times \begin{bmatrix} \Delta\theta_1 \\ \Delta\theta_2 \\ \Delta\omega_1 \\ \Delta\omega_2 \end{bmatrix} + \begin{bmatrix} 0 & 0 \\ 0 & 0 \\ \frac{1}{J_1} & 0 \\ 0 & \frac{1}{J_2} \end{bmatrix} \times \begin{bmatrix} \Delta T_w \\ \Delta T_e \end{bmatrix} \tag{2.11}$$

2.3 Permanent Magnet Synchronous Generator (PMSG) model

The main purpose of the PMSG is to generate electricity from the extracted mechanical energy from the wind by the rotating Turbine. Inside arrangement of PMSG, a permanent magnet mounted to the rotor is generating the rotor magnetic flux.

The main intention of this work is to make a model of the PMSG from its fundamental mathematical equations and understanding its behaviour upon a small amount of disturbance. The mathematical models of PMSGs and converter/inverter assemblies are formed using several assumptions, which are listed below [**19**], [**20**]

- The stator windings are placed sinusoidal along with the air-gap.
- No variations on rotor inductance due to stator slots with rotor position.
- Magnetic effect due to hysteresis and saturation is smaller hence not considered.
- Considered stator winding arrangement is symmetrical.
- Effect of damping windings is not included for calculations.
- Windings capacitances are negligible and the resistances are fixed (constant power loss).

We usually model PMSG in the rotor field reference Frame using d&q axis, where the q-axis 90 degree leads the d-axis when considered with the direction of rotation. It is said that the d-axis is magnetically centred to the north pole.

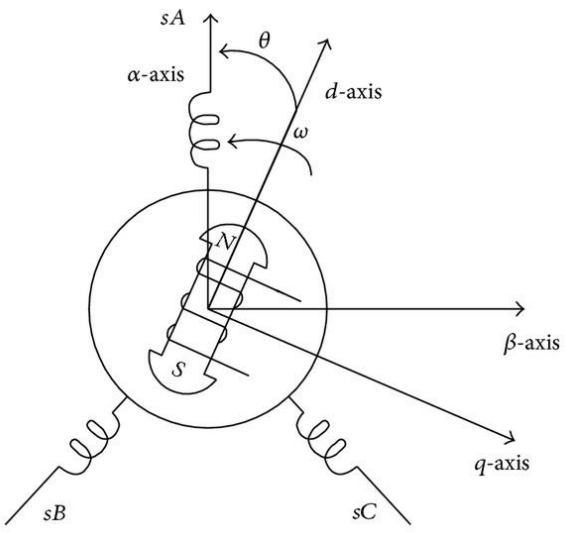

Figure 11 - Generator d-q axis representation

The stator voltage equations for the PMSG,

$$V_{ds} = -R_s i_{ds} - \omega_r \psi_{qs} + \dot{\psi}_{ds} \tag{2.12}$$

$$V_{qs} = -R_s i_{qs} + \omega_r \psi_{ds} + \dot{\psi}_{qs} \tag{2.13}$$

The flux linkages in the form of equations,

$$\psi_{ds} = -L_{ds} i_{ds} + \psi_{rd} \tag{2.14}$$

$$\psi_{qs} = -L_{qs} i_{qs} + \psi_{rq} \tag{2.15}$$

$$\psi_{rd} = \psi_{PM} \tag{2.16}$$

$$\psi_{rq} = 0 \tag{2.17}$$

Where,

ψ_{ds}/ψ_{qs} = flux linkages of d & q axis windings of stator
ψ_{rd}/ψ_{rq} = flux linkage of rotor winding against the d & qaxis
ψ_{PM} = rotating permanant magnet flux linkage(PM)
i_{ds}/i_{qs} = stator windings current of d & q axis
L_{ds}/L_{qs} = stator winding inductance against of d & q axis
np = pole pairs

By simplifying stator voltage equations yield to,

$$V_{ds} = \frac{-R_s}{L_{ds}}(\psi_{PM} - \psi_{ds}) - \omega_e \psi_{qs} + \dot{\psi}_{ds} \tag{2.18}$$

$$V_{qs} = -R_s(-\frac{\psi_{qs}}{L_{qs}}) + \omega_e \psi_{ds} + \dot{\psi}_{qs} \tag{2.19}$$

The simplified dq frame PMSG model is shown below.

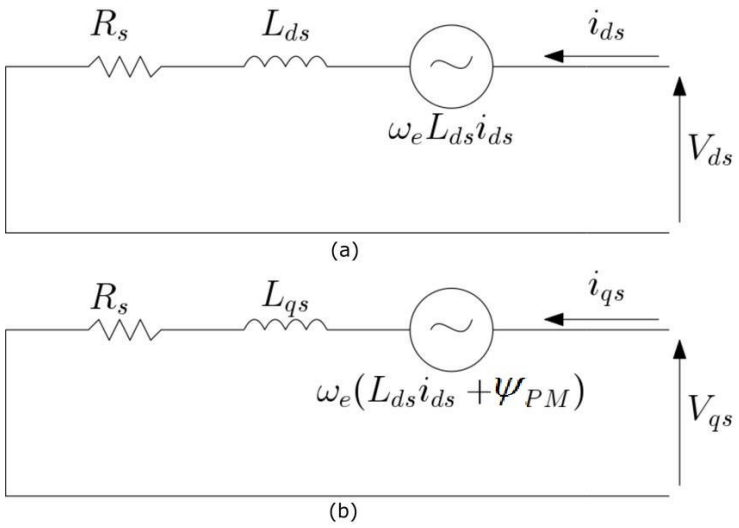

Figure 12- Equivalent circuits for d-and q axises

By linearizing the above equations, we can form the block in following form.

$$\Delta \dot{\boldsymbol{X}}_G = \boldsymbol{A}_G \Delta \boldsymbol{X}_G + \boldsymbol{B}_G \Delta \boldsymbol{u}_G \tag{2.20}$$

$$\begin{bmatrix} \Delta \dot{\psi}_{ds} \\ \Delta \dot{\psi}_{qs} \end{bmatrix} = \begin{bmatrix} -\frac{R_s}{L_{ds}} & \omega_b \\ -\omega_b & -\frac{R_s}{L_{qs}} \end{bmatrix} \times \begin{bmatrix} \Delta \psi_{ds} \\ \Delta \psi_{qs} \end{bmatrix} + \begin{bmatrix} 1 & 0 & \psi_{qs0} \\ 0 & 1 & \psi_{ds0} \end{bmatrix} \begin{bmatrix} \Delta V_{ds} \\ \Delta V_{qs} \\ \Delta \omega_e \end{bmatrix} \tag{2.21}$$

The electromagnetic torque developed by the PMSG is simplified using below equations.

$$T_e = \frac{3}{2} n_p \left(\psi_{ds} i_{qs} - \psi_{qs} i_{ds} \right) \tag{2.22}$$

$$T_e = \frac{3}{2} n_p \left(\psi_{PM} i_{qs} - (L_{ds} - L_{qs}) i_{ds} i_{qs} \right) \tag{2.23}$$

$$T_e = \frac{3}{2} n_p \psi_{PM} i_{qs} \tag{2.24}$$

L_{ds} and L_{qs} represents the stator windings inductance along with d&q axises respectively. Here we assumed a non-salient pole type PMSG for this research, hence the d&q axis inductances becomes equal by theory.

2.4 Generator Side Converter (GSC) model

PMSGs are mostly used together with full range back-to-back PWM converters because of their high fault riding through capability and grid voltage supporting facility. [**21**] This arrangement of wind plants consists of a wind turbine, a PMSG and two number of voltage source converters (VSCs). Two VSCs are named as Generator Side Converter (GSC) and Voltage Source Inverter (VSI). Here, GSC is at the generator side and VSI is at the AC power grid side. For GSCs there are two main controlling schemes available in the market namely; decoupled dq vector control and power signal feed-back control. Here, for this study power signal feedback control scheme is used for GSC.

In power signal feedback control scheme, turbine power which is calculated as per the Maximum Power Point Tracking (MPPT) method is fed as the input. To govern the electromagnetic torque_T_e, this study operates the q_axis current making the assumption of d_axis current becomes zero. [**22**] Vector control approach is used in control logic and space vector PWM is adopted in IGBT driver. X_1, X_2 and X_3 are intermediate state variables.

The GSC control schematic is displayed in Figure below. Using the MPPT function turbine power is provided as an input and with reference to the generator power, the error X_1 is produced. The error is forwarded through a PI controller block to produce

q -axis reference current. After comparing with generator q-axis current component error X_2 is generated. D_axis current is regulated to be minas possible to limit the reactive power produced.

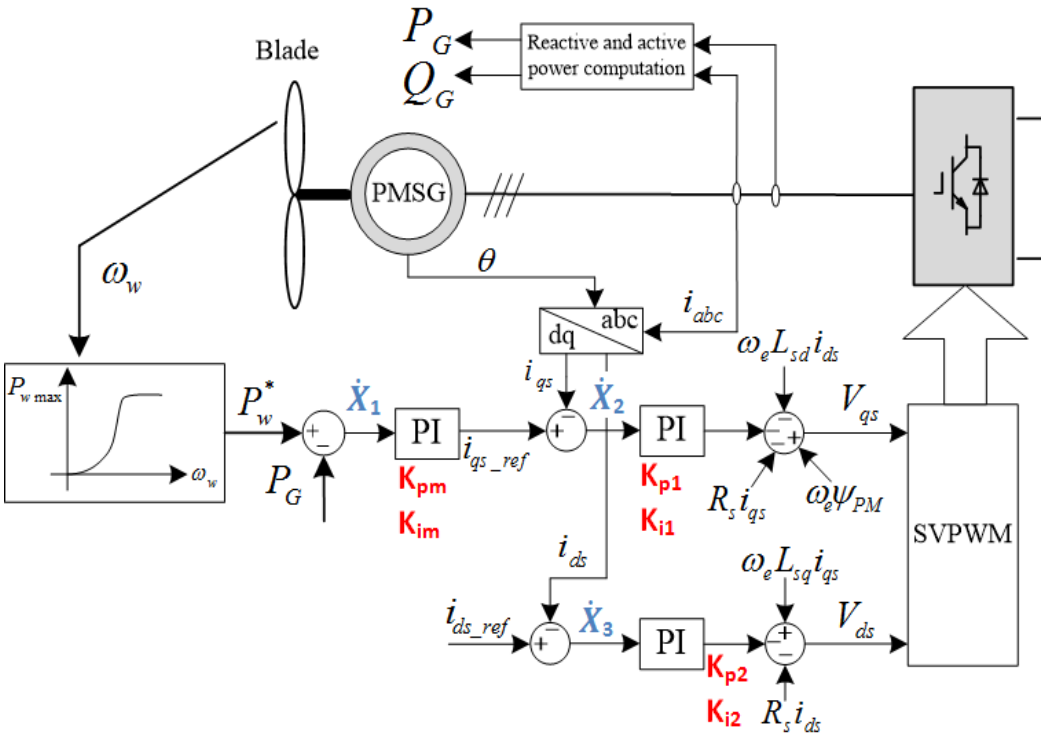

Figure 13 - Generator side converter representation

Dynamic equations for the system can be written as below.

$$i_{ds\_ref} = 0 \tag{2.25}$$

$$\dot{x}_1 = P_{w\_ref} - P_G \tag{2.26}$$

$$\dot{x}_2 = i_{qs\_ref} - i_{qs} \tag{2.27}$$

$$\dot{x}_3 = i_{ds\_ref} - i_{ds} \tag{2.28}$$

$$i_{qs\_ref} = K_{pm}\dot{x}_1 + K_{im}x_1 \tag{2.29}$$

$$V_{ds} = \omega_e L_{sq} i_{qs} - R_s i_{ds} - K_{p2}\dot{x}_3 - K_{i2}x_3 \tag{2.30}$$

$$V_{qs} = \omega_e \psi_{PM} - \omega_e L_{sd} i_{ds} - R_s i_{qs} - K_{p1}\dot{x}_2 - K_{i1}x_2 \tag{2.31}$$

By simplifying and linearizing the above equations, we can form the GSC block in following form.

$$\Delta \dot{\boldsymbol{X}}_{GSR} = \boldsymbol{A}_{GSR}\Delta \boldsymbol{X}_{GSR} + \boldsymbol{B}_{GSR}\Delta \boldsymbol{u}_{GSR} \tag{2.32}$$

$$\begin{bmatrix} \Delta \dot{x}_1 \\ \Delta \dot{x}_2 \\ \Delta \dot{x}_3 \end{bmatrix} = \begin{bmatrix} 0 & 0 & 0 \\ K_{im} & 0 & 0 \\ 0 & 0 & 0 \end{bmatrix} \times \begin{bmatrix} \Delta x_1 \\ \Delta x_2 \\ \Delta x_3 \end{bmatrix} + \begin{bmatrix} -i_{ds0} & -i_{qs0} & -u_{ds0} & -u_{qs0} & 1 & 0 \\ -K_{pm}i_{ds0} & -K_{pm}i_{qs0} & -K_{pm}u_{ds0} & -K_{pm}u_{qs0} & K_{pm} & 0 \\ 0 & 0 & 0 & -1 & 0 & 0 \end{bmatrix} \times \begin{bmatrix} \Delta V_{ds} \\ \Delta V_{qs} \\ \Delta i_{ds} \\ \Delta i_{qs} \\ \Delta P_{w\_ref} \\ \Delta \omega_e \end{bmatrix} \tag{2.33}$$

2.5 DC connecting link model

The generator and grid side converter transmit active and reactive power through the dc connecting link, which couples them. This primarily consists of a capacitor, so the dynamics are mainly governed by the capacitor.

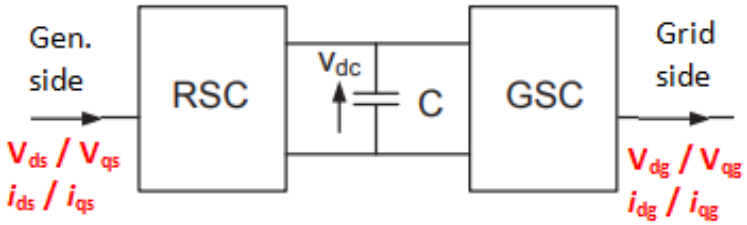

Figure 14 - DC link representation

The power loss in the converter is small compared to the power transfer through the converter. Here we make the assumption of no active power loss happens through the converters and do the calculations.

$$(Capacitor\_power) = (Generator\_power) - (Power\_delivered) \tag{2.34}$$

$$-(0.5 \times C \times V^2{}_{dc}) = (V_{ds}i_{ds} + V_{qs}i_{qs}) - (V_{dg}i_{dg} + V_{qg}i_{qg}) \tag{2.35}$$

By simplifying and linearizing the above equations, we can form the DC-link block in following form.

$$\Delta \dot{\boldsymbol{X}}_{dc} = \boldsymbol{A}_{dc}\Delta \boldsymbol{X}_{dc} + \boldsymbol{B}_{dc}\Delta \boldsymbol{u}_{dc} \tag{2.36}$$

$$[\dot{\Delta V}_{dc}] = [0] \times [\Delta V_{dc}] + \begin{bmatrix} i_{qg0} & i_{dg0} & u_{qg0} & u_{dg0} & -i_{qs0} & -i_{ds0} & -V_{qs0} & -V_{ds0} \end{bmatrix} \times \begin{bmatrix} \Delta V_{qg} \\ \Delta V_{dg} \\ \Delta i_{qg} \\ \Delta i_{dg} \\ \Delta V_{qs} \\ \Delta V_{ds} \\ \Delta i_{qs} \\ \Delta i_{ds} \end{bmatrix} \quad (2.37)$$

2.6 Voltage Source Inverter (VSI) model

Voltage Source Inverter (VSI) acts as the device which regulates the dc-link voltage to a constant value and produces zero reactive power output.

The VSI control schematic is illustrated in Figure below. Active power control is done through d_axis current and the reactive power control is done through q_axis current. DC link voltage is provided as an input and by comparing it with DC link voltage reference, the error X_4 is produced. The error is being directed through a PI controller to make d-axis reference current. By comparing it with actual d-axis current and passing through a PI controller d-axis voltage to the PWM controller is obtained. In a similar manner from the reactive power error q-axis voltage to the PWM controller is obtained.

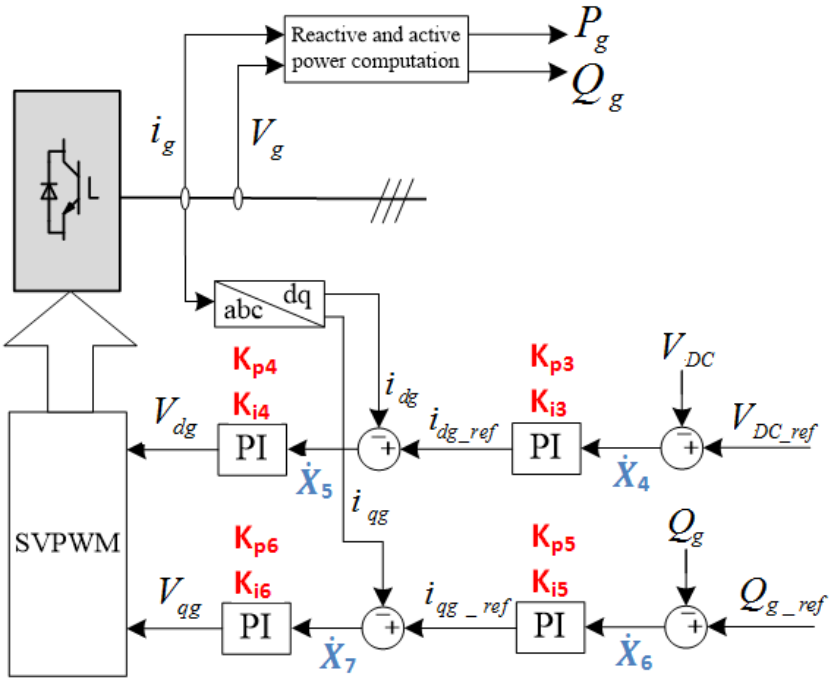

Figure 15 - Voltage source inverter model representation

Considering the dynamic model, following equations can be made.

$$\dot{x}_4 = V_{DC\_ref} - V_{DC} \tag{2.38}$$

$$\dot{x}_5 = i_{dg\_ref} - i_{dg} \tag{2.39}$$

$$\dot{x}_6 = Q_{g\_ref} - Q_g \tag{2.40}$$

$$\dot{x}_7 = i_{qg\_ref} - i_{qg} \tag{2.41}$$

$$i_{dg\_ref} = K_{p3}\dot{x}_4 + K_{i3}x_4 \tag{2.42}$$

$$V_{dg} = K_{p4}\dot{x}_5 + K_{i4}x_5 \tag{2.43}$$

$$i_{qg\_ref} = K_{p5}\dot{x}_6 + K_{i5}x_6 \tag{2.44}$$

$$V_{qg} = K_{p6}\dot{x}_7 + K_{i6}x_7 \tag{2.45}$$

By simplifying and linearizing the above equations, we can form the VSI block in following form.

$$\Delta\dot{\boldsymbol{X}}_{VSI} = \boldsymbol{A}_{VSI}\Delta\boldsymbol{X}_{VSI} + \boldsymbol{B}_{VSI}\Delta\boldsymbol{u}_{VSI} \tag{2.46}$$

$$\begin{bmatrix} \Delta\dot{x}_4 \\ \Delta\dot{x}_5 \\ \Delta\dot{x}_6 \\ \Delta\dot{x}_7 \end{bmatrix} = \begin{bmatrix} 0 & 0 & 0 & 0 \\ K_{i3} & 0 & 0 & 0 \\ 0 & 0 & 0 & 0 \\ 0 & 0 & K_{i5} & 0 \end{bmatrix} \times \begin{bmatrix} \Delta x_4 \\ \Delta x_5 \\ \Delta x_6 \\ \Delta x_7 \end{bmatrix} + \begin{bmatrix} 1 & 0 & -1 & 0 & 0 & 0 & 0 \\ K_{p3} & 0 & -K_{p3} & 0 & 0 & -1 & 0 \\ 0 & 1 & 0 & i_{gq0} & -i_{gd0} & -u_{gq0} & u_{gd0} \\ 0 & K_{p5} & 0 & K_{p5}i_{gq0} & -K_{p5}i_{gd0} & -K_{p5}u_{gq0} & K_{p5}u_{gd0} -1 \end{bmatrix} \times \begin{bmatrix} \Delta V_{DC\_ref} \\ \Delta Q_{g\_ref} \\ \Delta V_{DC} \\ \Delta V_{dg} \\ \Delta V_{qg} \\ \Delta i_{dg} \\ \Delta i_{qg} \end{bmatrix} \tag{2.47}$$

2.7 Transmission cable model

Here transmission line considered is a shielded cable which is in 33kV voltage range in Sri Lankan concept. Normally if we install a shielded cable, a compensation capacitor is added series to the cable in order to advance the power transfering capacity. For the ease of modelling, equivalent RLC circuit has made considering all the resistances, inductances and capacitances.

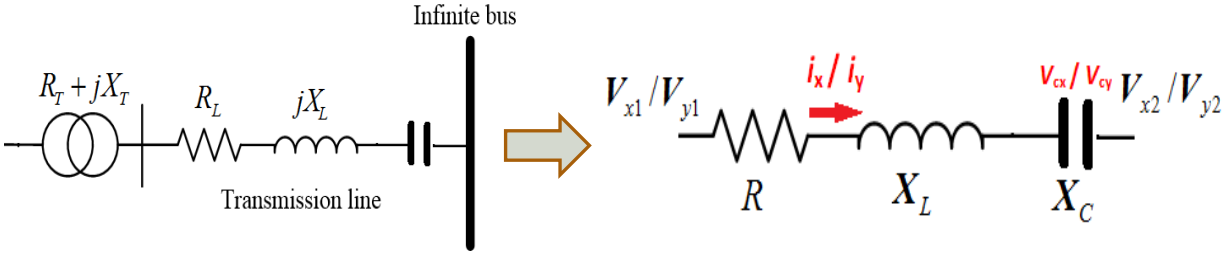

Figure 16 - Representation of transmission line

Voltages,

$$V_1 = L\frac{di}{dt} + R \times i + V_C + V_2 \tag{2.48}$$

By using dynamic phasors this can be written as,

$$(V_{x1} + jV_{y1})e^{jw_0 t} = L\frac{d\{(i_x + ji_y)e^{jw_0 t}\}}{dt} + R(i_x + ji_y)e^{jw_0 t} + (V_{Cx} + jV_{Cy})e^{jw_0 t} + (V_{x2} + jV_{y2})e^{jw_0 t} \tag{2.49}$$

$$(V_{x1} + jV_{y1}) = L * \frac{d(i_x + ji_y)}{dt} + (R + jw_0 L)(i_x + ji_y) + (V_{Cx} + jV_{Cy}) + (V_{x2} + jV_{y2}) \tag{2.50}$$

$$\frac{d(i_x + ji_y)}{dt} = \frac{1}{L}\left[(-Ri_x + w_0 Li_y + V_{x1} - V_{Cx} - V_{x2}) + (jw_0 Li_x - jRi_y + jV_{y1} - jV_{Cy} - jV_{y2})\right] \tag{2.51}$$

Currents,

$$i = -i_C \tag{2.52}$$

$$i = -C\frac{dV_C}{dt} \tag{2.53}$$

By using dynamic phasors this can be written as,

$$(i_x + ji_y)e^{jw_0 t} = -C\frac{d\{(V_{Cx} + jV_{Cy})e^{jw_0 t}\}}{dt} \tag{2.54}$$

$$(i_x + ji_y) = -C\frac{d(V_{Cx} + jV_{Cy})}{dt} - (jw_0C)(V_{Cx} + jV_{Cy}) \tag{2.55}$$

$$\frac{d(V_{Cx} + jV_{Cy})}{dt} = -\frac{1}{C}(i_x + ji_y) - (jw_0)(V_{Cx} + jV_{Cy}) \tag{2.56}$$

By simplifying and linearizing the above equations, we can form the Transmission line block in following form.

$$\Delta\dot{\boldsymbol{X}}_{RLC} = \boldsymbol{A}_{RLC}\Delta\boldsymbol{X}_{RLC} + \boldsymbol{B}_{RLC}\Delta\boldsymbol{u}_{RLC} \tag{2.57}$$

$$\begin{bmatrix} \Delta\dot{i}_x \\ \Delta\dot{i}_y \\ \Delta\dot{V}_{cx} \\ \Delta\dot{V}_{cy} \end{bmatrix} = \begin{bmatrix} -\omega_b R_{TL}/X_{TL} & \omega_b & -\omega_b/X_{TL} & 0 \\ -\omega_b & -\omega_b R_{TL}/X_{TL} & 0 & -\omega_b/X_{TL} \\ -\omega_b X_C & 0 & 0 & \omega_b \\ 0 & -\omega_b X_C & -\omega_b & 0 \end{bmatrix} \times \begin{bmatrix} \Delta i_x \\ \Delta i_y \\ \Delta V_{cx} \\ \Delta V_{cy} \end{bmatrix} + \begin{bmatrix} \omega_b/X_{TL} & 0 & -\omega_b/X_{TL} & 0 \\ 0 & \omega_b/X_{TL} & 0 & -\omega_b/X_{TL} \\ 0 & 0 & 0 & 0 \\ 0 & 0 & 0 & 0 \end{bmatrix} \times \begin{bmatrix} \Delta V_{x1} \\ \Delta V_{y1} \\ \Delta V_{x2} \\ \Delta V_{y2} \end{bmatrix} \tag{2.58}$$

2.8 Final model

By combining the blocks explained and modelled above, we can create the final model of the wind power plant. As one block's output becomes the input of another block, linearized equations are needed to be expanded and solved.

Following is a summary of blocks with their inputs and outputs.

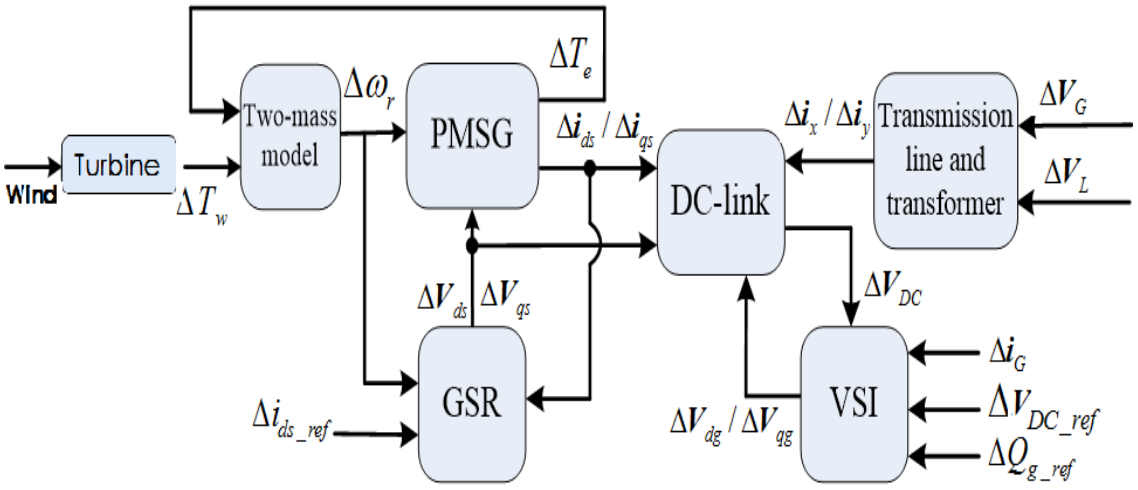

Figure 17 - Inputs/outputs of blocks which creates the wind plant

There are 18 numbers of state variables which represent each component/block of the wind power plant. As we combine all the blocks together these 18 state variables become the state variables of total wind power plant system.

Following is a summary of state variables of the system.

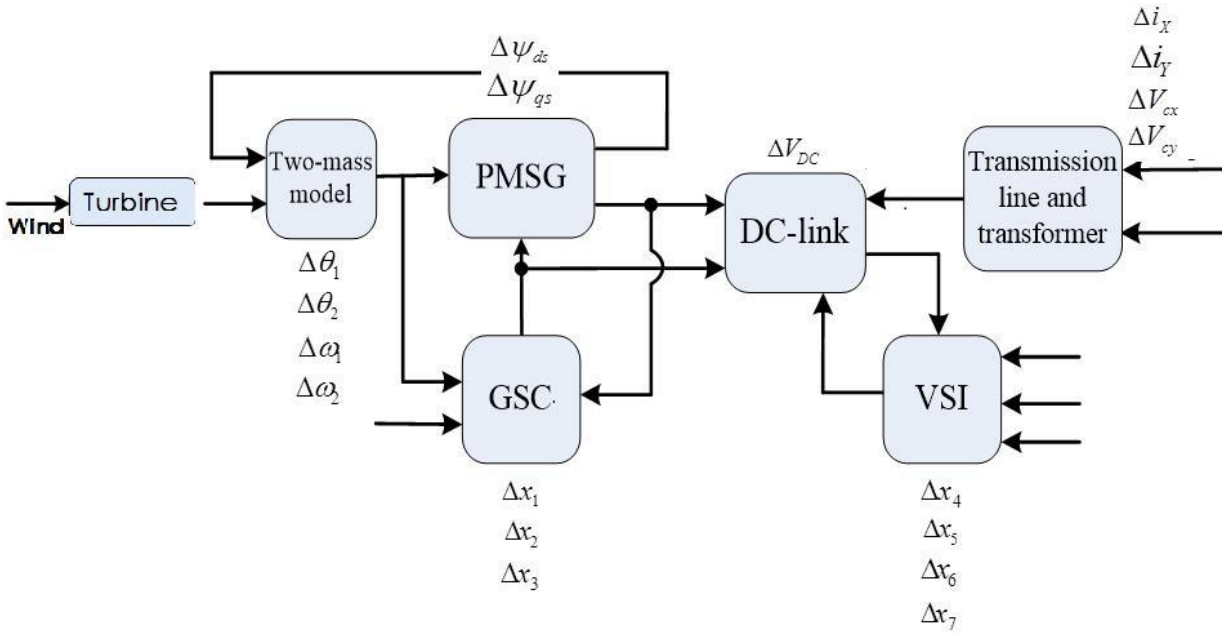

Figure 18 - Summary of state variables

After simplifying final model can be obtained in following form.

$$\Delta\dot{\boldsymbol{X}}_{\boldsymbol{FINAL}} = \boldsymbol{A}_{\boldsymbol{FINAL}}\Delta\boldsymbol{X}_{\boldsymbol{FINAL}} + \boldsymbol{B}_{\boldsymbol{FINAL}}\Delta\boldsymbol{u}_{\boldsymbol{FINAL}} \tag{2.59}$$

There,

$$\Delta\boldsymbol{X}_{\boldsymbol{FINAL}} = \left[\Delta\theta_1 \;\; \Delta\theta_2 \;\; \Delta\omega_1 \;\; \Delta\omega_2 \;\; \Delta\psi_{ds} \;\; \Delta\psi_{qs} \;\; \Delta x_1 \;\; \Delta x_2 \;\; \Delta x_3 \;\; \Delta V_{DC} \;\; \Delta x_4 \;\; \Delta x_5 \;\; \Delta x_6 \;\; \Delta x_7 \;\; \Delta i_x \;\; \Delta i_y \;\; \Delta V_{cx} \;\; \Delta V_{cy}\right]^T$$

$$\Delta U_{Final} = \left[\Delta T_w \;\; \Delta i_{ds\_ref} \;\; \Delta V_{DC\_ref} \;\; \Delta Q_{g\_ref} \;\; \Delta V_L\right]^T$$

$$\boldsymbol{A}_{FINAL} = \begin{bmatrix} \boldsymbol{A}_M & \boldsymbol{A}_{G\_M} & \boldsymbol{0} & \boldsymbol{0} & \boldsymbol{0} & \boldsymbol{0} \\ \boldsymbol{A}_{M\_G} & \boldsymbol{A}'_G & \boldsymbol{A}_{GSR\_G} & \boldsymbol{0} & \boldsymbol{0} & \boldsymbol{0} \\ 0 & \boldsymbol{A}_{G\_GSR} & \boldsymbol{A}'_{GSR} & \boldsymbol{A}_{DC\_GSR} & \boldsymbol{0} & \boldsymbol{0} \\ \boldsymbol{A}_{M\_DC} & \boldsymbol{A}_{G\_DC} & \boldsymbol{A}_{GSR\_DC} & \boldsymbol{A}'_{DC} & \boldsymbol{A}_{VSI\_DC} & \boldsymbol{A}_{RLC\_DC} \\ \boldsymbol{0} & \boldsymbol{0} & \boldsymbol{0} & \boldsymbol{A}_{DC\_VSI} & \boldsymbol{A}_{VSI} & \boldsymbol{A}_{RLC\_VSI} \\ \boldsymbol{0} & \boldsymbol{0} & \boldsymbol{0} & \boldsymbol{A}_{DC\_RLC} & \boldsymbol{A}_{VSI\_RLC} & \boldsymbol{A}'_{RLC} \end{bmatrix}$$

Detailed model is included in Appendix B.

Chapter Summary

This chapter carried out a detailed method of developing a linearized model for Type 4 wind power plant system. Dynamic phasors approach was used in modelling the transmission line as series RLC circuits are involved. Next chapter will bring out the validation and results/analysis of the model created in this chapter.

3 RESULTS AND ANALYSIS

In the above chapter a descriptive way of developing a small signal stability model for a wind power plant is presented. It is a generic model which can be applied for any type 4 wind power plant which consists of a permanent magnet synchronous generator, fully rated converter/inverter assembly and shielded cable as a transmission line. Here, in this chapter the model validation and a sensitivity analysis using 2MVA test system will be presented.
2MVA test system specifications are presented in **Annexure 01**. A point where test system runs stable at full load is selected as the test point for the analysis.

3.1 Model stability

As described in the introduction, using small signal stability analysis we can represent the linearized dynamic model of a test system in following format.

$$\Delta\dot{\boldsymbol{X}} = \boldsymbol{A}\Delta\boldsymbol{X} + \boldsymbol{B}\Delta\boldsymbol{U} \tag{3.1}$$

There matrixes X = states variables, A = state controls, U = system inputs, B = input controls will be represented. By analysing the eigenvalues of matrix A we can comment on the stability/behaviour of the power system.

Eigenvalues & Eigenvectors

If we consider a matrix, the eigenvalues are represented by the scalar parameter λ (the values of λ matrix), where λ got non-trivial solutions (i.e. other than Θ=0) to the equation, [**7**]

$$A\theta = \lambda\theta \tag{3.2}$$

Where,

A = an $n \times n$ matrix (real for a physical system such as a power system)
Θ = an $n \times 1$ vector

To find the eigenvalues, equation 3.2 can be re-written in the form,

$$(A - \lambda I)\theta = 0 \tag{3.3}$$

For a non-trivial solution,

$$\det(A - \lambda I) = 0 \tag{3.4}$$

Expansion of the determinant gives the characteristic solution. The ***n*** number of solutions comes for the λ ($\lambda = \lambda_1, \lambda_2, \lambda_3 \ldots \lambda_n$) are the **Eigenvalues** of matrix **A**. Eigen values can be real values or complex values.

For any given eigenvalue λ, the column vector Θ_i with n number of columns, which fulfils equation 3.2 is identified as the **right eigenvector** of matrix A. in the same manner, the vector ϕ_i with n no of rows, which satisfies

$$\phi A = \lambda \phi \tag{3.5}$$

is said to be the **left eigenvector** of the matrix A.

Stability analysis criteria

As per the Lyapunov's first criteria, the stability of a non-linear system can be predicted using the roots of the characteristic equation of the system. (eigenvalues of matrix A); [**7**]

I. If the eigenvalues got real negative parts, it is said that the system is asymptotically stable.
II. If a single eigenvalue got a positive real part, it is said that the system is unstable.
III. If eigenvalues got real parts which are equal to zero, it is said that stability of the system is difficult to be predicted using first approximations.

Oscillation frequency & Oscillation modes

As mentioned above some eigenvalues are a combination of real and imaginary parts. These complex pairs of eigenvalues are called **Oscillation modes** and can be written in the form of,

$$\lambda = \sigma \pm j\omega \tag{3.6}$$

We can calculate the damping ratio using real part of the eigenvalue and the frequency of oscillation using the imaginary part of the eigenvalue.

$$\textit{o}\text{scillation}\ \ \textit{frequency}\,(\text{f}) = \frac{\omega}{2\pi} \tag{3.7}$$

$$\textit{d}\text{amping}\ \textit{r}\text{atio}\ (\varsigma) = \frac{-\sigma}{\sqrt{\sigma^2 + \omega^2}} \tag{3.8}$$

Stability analysis of 2MVA test system

Linearized 2MVA test system model was created using the system model developed in chapter 2. (Test system data/specifications are provided on Annexure 01) Calculations carried out using the developed system model were done on **Matlab** software platform.

Results obtained are displayed on table 01 below.

	Eigenvalues	Oscillation frequency (Hz)	oscillation mode no:
λ1, λ2	-0.0000 ±12.1275i	1.9301	1
λ3, λ4	-0.2814 ±10.4068i	1.6563	2
λ5, λ6	-0.0813 ± 2.0494i	0.3262	3
λ7, λ8	-0.0014 ± 1.1146i	0.1774	4
λ9	-0.2421	0	
λ10	-0.7711	0	
λ11	-0.6667	0	
λ12	-0.3518	0	
λ13, λ14	-0.1924 ± 0.0242i	0.0039	5
λ15, λ16	-0.0036 ± 0.0000i	0.0001	6
λ17	-0.0000	0	
λ18	-0.0000	0	

Table 1 - Eigenvalues of the 2MVA test system

It can be clearly identified 6 no of oscillation modes in the system. We can say that system is getting stable after facing to a small disturbance as real-parts of all eigenvalues are negative. All the values are rounded to four decimal places. Hence, λ_{17} and λ_{18} are displayed zeroes as the got very small real components.

Plotting a variation of state variable

Using Matlab software, percentage input can be provided to the input matrix and output can be monitored. Here in this study generator rotational speed (ω_2) was selected as the monitoring output parameter and the system was simulated giving percentage input to the wind turbine power. Variance observed is below on figure 19.

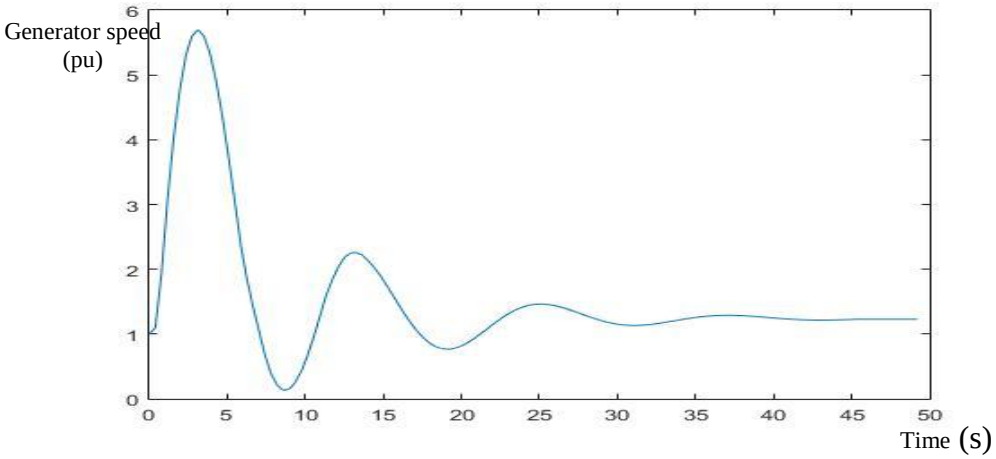

Figure 19 - Generator speed after small disturbance

By observing the graph it is clearly visible that, the system is getting stable after a short period of time when it is subjected to a small disturbance.

3.2 Model validation using PSCAD

Same, 2MVA test system was modelled on PSCAD software platform using electrical, electronic and mechanical component models in the software to simulate the system.

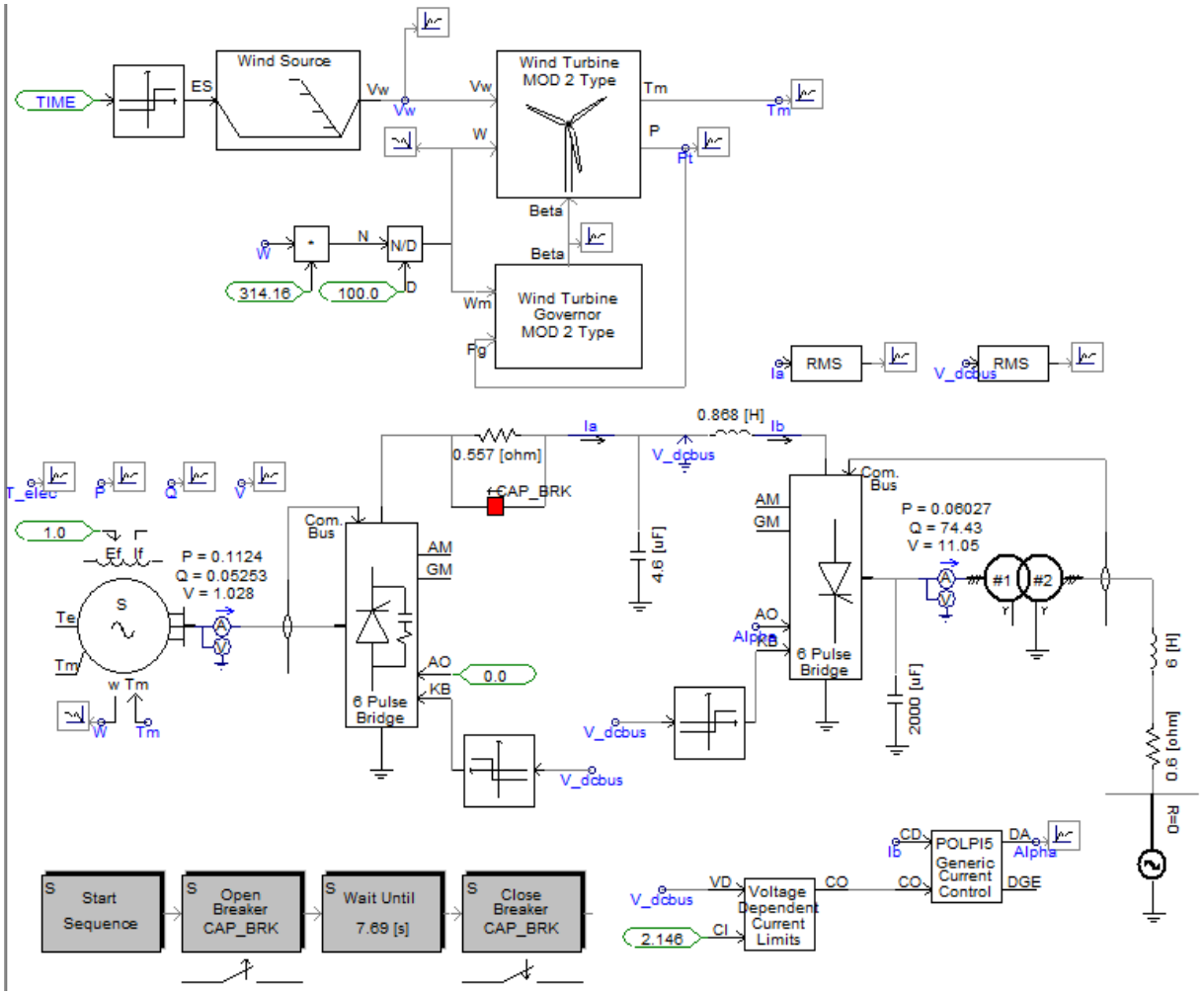

Figure 20 - PSCAD simulation model

In a similar manner performed in Matlab software platform small variation to the wind speed is proved and generator rotational speed (ω_2) variance is monitored/ plotted.

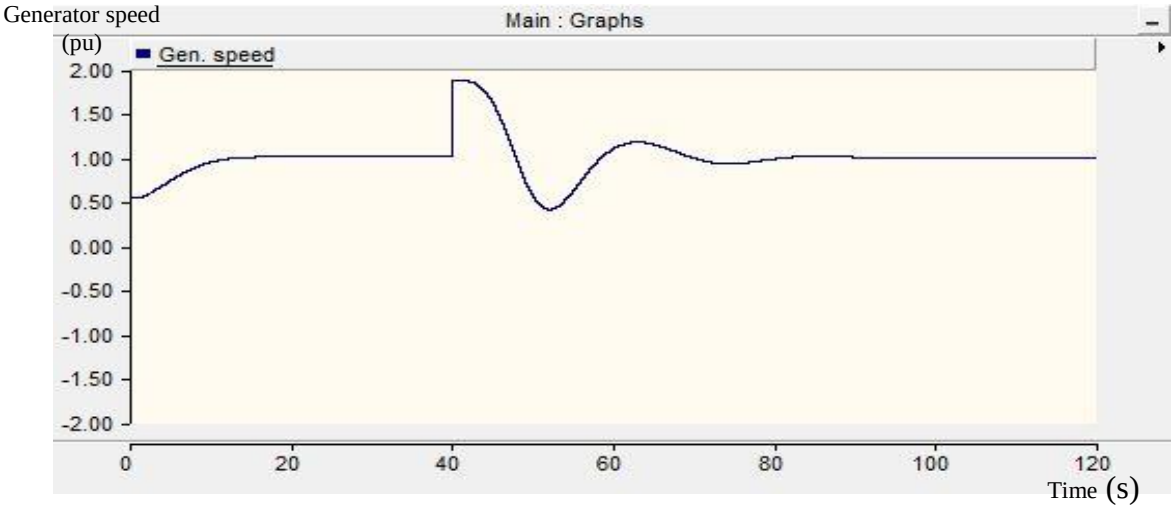

Figure 21 - Generator speed variation

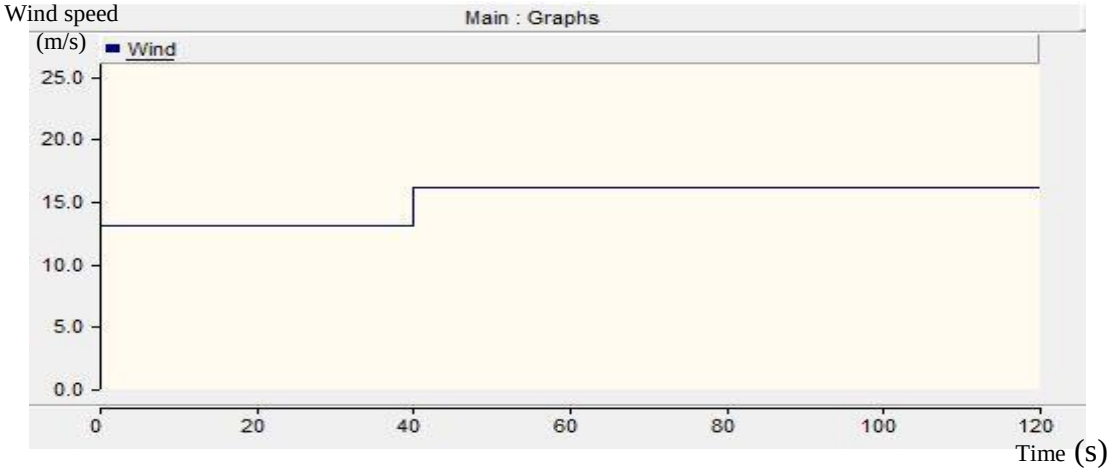

Figure 22 - Wind speed variation

From the graphs it is clearly visible that after a small disturbance system gets stable within short period of time.

3.3 Sensitivity analysis

The sensitivity of the eigenvalue λ_i to the corresponding element a_i is studied through the sensitivity analysis. Here we use participation factors for measuring this sensitivity.

Participation factors

Participation factor gives a measurement of the amount of relative participation of state variables to the oscillation mode and vice versa. Multiplication of right eigenvector matrix and the left eigenvector matrix produces the participation matrix, which includes the participation factors.

$$P_{ki} = \theta_{ki}\phi_{ik} \tag{3.9}$$

P_{ki} = participation factor
Θ_{ki} = k^{th} entry of the right eigenvector Θ_i
ϕ_{ik} = k^{th} entry of the right eigenvector ϕ_i

The participation factors which got higher values indicates; those oscillation modes are highly sensitive or highly influenced by the corresponding state variables.

Sensitivity analysis of 2MVA test system using participation factors

Using Matlab software platform following participation factors corresponding to the 6 oscillation modes identified in Table 01, were calculated.

	State variables	λ1, λ2	λ3, λ4	λ5, λ6	λ7, λ8	λ11, λ12	λ15, λ16
Drive train	$\Delta\theta_1$	0.0472	0.0000	0.0000	0.0000	0.0000	0.0000
	$\Delta\theta_2$	**0.4528**	0.0000	0.0000	0.0000	0.0000	0.0000
	$\Delta\omega_1$	0.0472	0.0000	0.0000	0.0000	0.0000	0.0000
	$\Delta\omega_2$	**0.4528**	0.0000	0.0000	0.0000	0.0000	0.0000
Generator	$\Delta\psi_{ds}$	0.0000	0.0000	0.0000	0.0000	0.0000	0.0000
	$\Delta\psi_{qs}$	0.0000	0.0000	0.0000	0.0000	**1.0848**	0.0000
Generator side converter	Δx_1	0.0000	0.0000	0.0000	0.0000	0.2113	0.0000
	Δx_2	0.0000	0.0000	0.0000	0.0000	0.8735	0.0000
	Δx_3	0.0000	0.0000	0.0000	0.0000	0.0000	0.0000
DC Link	Δu_{DC}	0.0000	**0.5034**	0.0001	0.0008	0.0000	0.0000
Grid side inverter	Δx_4	0.0000	**0.4946**	0.0001	0.0002	0.0000	0.0001
	Δx_5	0.0000	0.0392	0.0271	0.0005	0.0000	0.0000
	Δx_6	0.0000	0.0000	0.0000	0.0001	0.0000	**0.9964**
	Δx_7	0.0000	0.0020	0.0143	0.0034	0.0000	0.0117
Transmission line	Δi_{Lx}	0.0280	0.0028	**0.5545**	0.0494	0.0000	0.0001
	Δi_{Ly}	0.0010	0.0351	**0.5669**	0.0483	0.0000	0.0092
	ΔV_{cx}	0.0000	0.0001	0.0512	**0.5525**	0.0000	0.0009
	ΔV_{cy}	0.0000	0.0001	0.0515	**0.5517**	0.0000	0.0000

Table 2 - Partcipation factors

Following points can be observed from the study.

Oscillations dominated by state variables related to power electronics

- Oscillation mode of λ_3, λ_4 which is highly depend on DC-link voltage and X_4 intermediate-variable of the VSI .
- Oscillation mode of λ_{15}, λ_{16} which is highly influenced by X_6 intermediate-variable of VSI .

Oscillations dominated by state variables related to transmission line

- Oscillation mode of λ_5, λ_6 which is highly influenced by the inducter current passing through the shielded cable/Transmission line. (both x-axis and y-axis components)
- Oscillation mode of λ_7, λ_8 which is highly influenced by the voltage of series-compansation capacitor. (both x-axis and y-axis components)

Oscillations dominated by state variables related to generator and drive train

- Oscillation mode of λ_1, λ_2 which is highly influenced by generator rotor speed ω_2 and the generator rotor twist angle θ_2.
- Oscillation mode of λ_{11}, λ_{12} which is highly depend on q-axis element of the stator flux ψ_{qs}.

Chapter summary

This chapter contains a detailed analysis of a 2MVA test system using the wind turbine model created in chapter 2. Analysis includes a model validation, system stability analysis and a sensitivity analysis using participation factors. Dominant oscillations introduced to the grid are identified by the later mentioned sensitivity analysis.

4 CONCLUSIONS AND FUTURE DIRECTIONS

4.1 Conclusions

Wind power plays a major role in renewable energy sector as it can be easily harvested and widely available same as the solar power. Converting wind energy to electricity is a field which is continuously developing. Different wind turbine-generator topologies are introduced time to time in order to maximize energy harvesting and gain more control in power generation. This thesis discusses about a type-4 wind turbine-generator model arrangement, which is considered as the latest technology available.

Wind power is an intermittent source and lot of fluctuations are there even for a small period of time considered. Also wind power to electricity conversion involves lot of mechanical and power electronic appliances. Due to these reasons transient formation is possible from a disturbance to the system. Hence detailed and complete studies are needed on power system stability when we add more and more wind plants to the grid network.

Small signal stability analysis is the most known conventional method of analysing the power system stability which falls in to the category of electromechanical transient analysis. Modern software based stability analysing techniques are electromagnetic transient analysis type; hence more range of power system transients can be studied. In this research dynamic phasors are used in transmission line modelling and generator stator flux is used in generator modelling, together with conventional small signal stability analysis. Therefore it can be considered as a study beyond electromechanical transient analysis, more towards electromagnetic transient analysis side.

One of the key-objectives of this study/thesis was to develop a mathematical model for the type 4 wind plant as it can be used on future studies regardless of capacity/power. So detailed description is provided from selecting the blocks to be modelled up to linearization and formation of $\dot{\mathbf{x}}=\mathbf{Ax}+\mathbf{Bu}$ type system model. A sample analysis was carried out on a 2MVA test system to identify dominant oscillations introduced by plant to the grid.

4.2 Future Directions

This research is limited to a single type 4 wind power plant connected to an infinite bus in order to develop the small signal stability model for the wind plant. But normally there are more than one unit at a place which forms a wind farm. It is difficult to study all the plants one by one in small signal stability analysis. Solution to this problem is to aggregate all the wind turbine-generator units into an equivalent turbine and generator and use it in the system simulation. [**31**], [**32**]

When aggregating the units, the inertia of an individual unit is scaled-up by the total count of units in the wind power farm while scaling down the winding resistances and the inductances by the same amount. The MVA rating of a unit is also scaled up. Therefore, the per unit inertia, resistance and the inductance of the aggregated wind power plant are equal to the corresponding quantities of an individual unit. Also, the converters and the converter transformer ratings are scaled up in the aggregated wind power plant. For example if a wind power plant consist of 100 2 MVA wind turbine-generator units with a 0.6 MVA converter transformer, the size of the aggregated wind power plant would be 200 MVA with a 60 MVA converter transformer.

The AC network or the grid is also needed to be modelled with dynamic phasors approach. The method described in modelling transmission line can be adopted here. After combining wind farm and the network, a full system model can be created and further studies can be carried out considering the nodal voltages and currents.

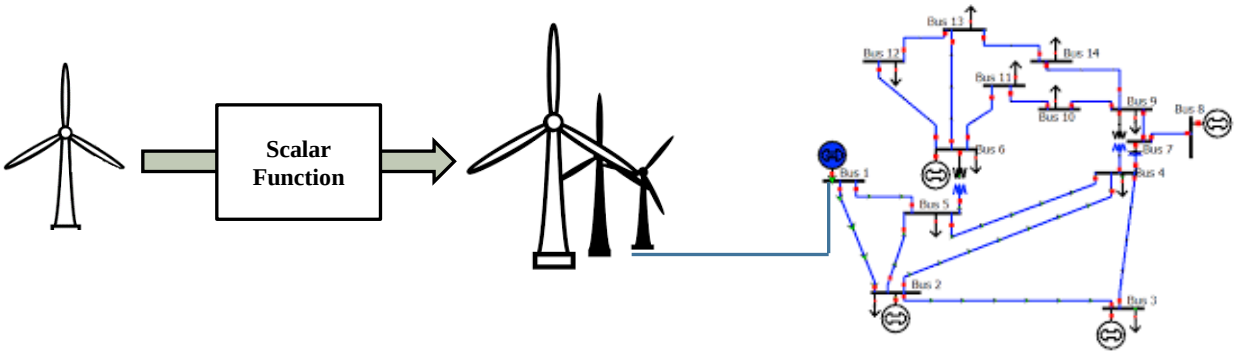

Figure 23 - Future scope

5 REFERENCES

[1] Thomas Ackermann, "Wind power in power systems," Chichester, 2005.

[2] [Online]. https://wwindea.org/blog/2018/02/12/2017-statistics/

[3] [Online].http://www.geni.org/globalenergy/library/renewable-energy-resources/world/asia/wind-asia/wind-srilanka.shtml

[4] [Online]. http://www.windpower.lk/

[5] CEB, "Long term generation plan 2018-2037," Ceylon Electricity Board, 2017.

[6] ABB, "Technical application papers no.13: Wind power plants," , Tech. Rep., ABB, 2011.

[7] Prabha Kundur, *Power system stability and control*, 1st ed.: MacGraw-Hill, 1994.

[8] Don Hiranya Ravipriya Suriyaarachchi, "Sub-synchronous Interactions in a Wind Integrated Power System," The Department of Electrical and Computer Engineering, The University of Manitoba, July 2014.

[9] IEEE subsynchronous working group, "Readers guide to subsynchronous resonance," IEEE Trans. Power Syst., vol. 7, no. 1, pp. 150–157 Feb. 1992.

[10] B. L. Agrawal, and J. E. Van Ness P. M. Anderson, "Subsynchronous resonance in power systems," IEEE Press, 1990.

[11] D. P. Sen Gupta, and K. R. Padiyar M. A. Pai, "Small Signal Analysis of Power systems," Alpha Science International, 2004.

[12] IEEE Commitee Report, "First benchmark model for computer simulation of subsynchronous resonance," IEEE Trans. Power App. Syst., vol. PAS-96, no. 5,pp. 1565–1572 Sep./Oct. 1977.

[13] L.Agquist, and H.P. Nee N. Johansson, "A comparison of different frequency scanning methods for study of subsynchronous resonance," IEEE Trans. Power Syst., vol. 26, no. 1, pp. 356–363 Feb. 2011.

[14] H. W. Dommel, "Digital computer solution of electromagnetic transients in single-and multi-phase networks," IEEE Trans. Power App. Syst., vol. PAS-88 pp. 388–399 April 1969.

[15] K. R. Padiyar, "Analysis of Subsynchronous Resonance in Power Systems," Kluwer Academic Publishers, 1999.

[16] Chandana Karawita, "HVDC Interaction Studies IJsing Small Signal Stability Assessment," The University of Manitoba, Manitoba, Canada, A dissertation submitted for Doctor of Philosophy April 2009.

[17] N. Jenkins, J. Ekanayake, P. Cartwright, and M. Hughes O. Anaya-Lara, "Wind energy generation modelling and control," Wiley, UK, 2009.

[18] " MATLAB R2007b Documentation.," The MathWorks Inc.,.

[19] H. Polinder, and W. L. Kling J. G. Slootweg, "Dynamic modeling of a wind turbine with doubly fed induction generator," Proc. IEEE PowerEng. Soc. Summer Meeting, Vancouver, BC, Canada, , Jul. 15-19, 2001.

[20] L. Holdsworth, X. Wu, and N. Jenkins J. B. Ekanayake, "Dynamic modeling of doubly fed induction generator wind turbines," IEEE Trans. Power Syst., vol.18, no. 3, pp. 803

[21] S. Auddy, and Y. Semsedini R. K. Varma, "Mitigation of subsynchronous resonancein a series-compensated wind farm using FACTS controllers," IEEE Trans. Power Del., vol. 23, no. 3, pp. 1645

[22] R. Kavasseri, Z. L. Miao, and C. Zhu L. Fan, "Modeling of DFIG-based wind farms for SSR analysis," IEEE Trans. Power Del., vol. 25, no. 4, pp. 2073

[23] F. Mei, "Small-signal modelling and analysis of Doubly-Fed Induction Generators in wind power applications," Imperial college, London, Phd Thesis 2008.

[24] N. Jenkins, J. Ekanayake, P. Cartwright, and M. Hughes O. Anaya-Lara, "Wind Energy Generation Modelling and Control," Wiley, UK, 2009.

[25] H. Li and Z. Chen, "Transient stability analysis of wind turbines with induction generators considering blades and shaft flexibility," 33rd Annual Conference of the IEEE Industrial Electronics Society (IECON), Taipei, Taiwan, Nov. 5-8, 2007.

[26] U. D. Annakkage, F. M. Hughes, and A. M. Gole N. Kshatriya, "Optimized partial eigenstructure assignment-baseddesign of a combined PSS and active damping controller for a DFIG," IEEE Trans. Power Syst., vol. 25, no. 2, pp.866

[27] 1.C. Burgos and L. Amalte L. Rodriguez, "Sistemas E6licos de Produccion de

Energia Electrica.," Madrid, 2003.

[28] C. Krause, "Analysis of electric machinery," United States of America, 2nd Edition 2002.

[29] Zhenbin, et al Zhang, "Encoderless model predictive control of back-to-back converter direct-drive permanent-magnet synchronous generator wind turbine systems," Power Electronics and Applications (EPE), 2013 15th European Conference on. IEEE, 2013.

[30] Wen-Chang Lin, and Xuan-Khoa Le Chia-Nan Wang, "Modelling of a PMSG Wind Turbine with Autonomous Control," Mathematical Problems in Engineering, Volume 2014, Article ID 856173, 9 pages.

[31] F. Jurado, and J. R. Saenz L. M. Fern´andez, "Aggregated dynamic model for wind farms with doubly fed induction generator wind turbines," Renewable Energy, vol. 33, no. 1, pp. 129–140 Jan. 2008.

[32] O. Anaya-Lara, G. Bathurst, and N. Jenkins, A. Shafiu, "Aggregated wind turbine models for power system dynamic studies," Wind Engineering, vol. 30, no. 3, pp. 171–186 May 2006.

6 Appendix

6.1 Appendix A – test system values

Turbine

C_p=0.45, R=37.75m, wind $speed_{rated}$ = 13m/s

Drive train

J_1=6.2506×106 kgm^2, J_2=6.511×105 kgm^2, K_{12}=8.673×107 Nm/rad, D_1=1.80 p.u., D_2=0.8 p.u., D_{12}=0.

Generator

n_p=24, P=1.6MW, f=50Hz, L_d=L_q=0.45 p.u, R_s=0.067p.u, ψ_{PM}=1.05 p.u..

Converter/Inverter

K_{pm}=0.2, K_{im}=0.3; K_{p1}=0.001, K_{i1}=0.01; Kp2=0.3, K_{i2}=70; K_{p3}=0.05, K_{i3}=20; K_{p4}=6.5, Ki4=50; K_{p5}=0.03, K_{i5}=0.01; K_{p6}=17, K_{i6}=4.

Line and t/f

R_T=0.007p.u., X_T=0.0440 p.u., R_L=0.840 p.u., X_L=8.402 p.u., X_C=0.851 p.u..

6.2 Appendix B – Final wind plant model

$$\Delta \dot{\boldsymbol{X}}_{\boldsymbol{FINAL}} = \boldsymbol{A}_{\boldsymbol{FINAL}} \Delta \boldsymbol{X}_{\boldsymbol{FINAL}} + \boldsymbol{B}_{\boldsymbol{FINAL}} \Delta \boldsymbol{u}_{\boldsymbol{FINAL}}$$

$$\Delta \boldsymbol{X}_{\boldsymbol{FINAL}} = \begin{bmatrix} \Delta\theta_1 & \Delta\theta_2 & \Delta\omega_1 & \Delta\omega_2 & \Delta\psi_{ds} & \Delta\psi_{qs} & \Delta x_1 & \Delta x_2 & \Delta x_3 & \Delta V_{DC} & \Delta x_4 & \Delta x_5 & \Delta x_6 & \Delta x_7 & \Delta i_x & \Delta i_y & \Delta V_{cx} & \Delta V_{cy} \end{bmatrix}^T$$

$$\Delta U_{Final} = \begin{bmatrix} \Delta T_w & \Delta i_{ds\_ref} & \Delta V_{DC\_ref} & \Delta Q_{g\_ref} & \Delta V_L \end{bmatrix}^T$$

$$\boldsymbol{A}_{FINAL} = \begin{bmatrix} \boldsymbol{A}_M & \boldsymbol{A}_{G\_M} & \boldsymbol{0} & \boldsymbol{0} & \boldsymbol{0} & \boldsymbol{0} \\ \boldsymbol{A}_{M\_G} & \boldsymbol{A}'_G & \boldsymbol{A}_{GSR\_G} & \boldsymbol{0} & \boldsymbol{0} & \boldsymbol{0} \\ 0 & \boldsymbol{A}_{G\_GSR} & \boldsymbol{A}'_{GSR} & \boldsymbol{A}_{DC\_GSR} & \boldsymbol{0} & \boldsymbol{0} \\ \boldsymbol{A}_{M\_DC} & \boldsymbol{A}_{G\_DC} & \boldsymbol{A}_{GSR\_DC} & \boldsymbol{A}'_{DC} & \boldsymbol{A}_{VSI\_DC} & \boldsymbol{A}_{RLC\_DC} \\ \boldsymbol{0} & \boldsymbol{0} & \boldsymbol{0} & \boldsymbol{A}_{DC\_VSI} & \boldsymbol{A}_{VSI} & \boldsymbol{A}_{RLC\_VSI} \\ \boldsymbol{0} & \boldsymbol{0} & \boldsymbol{0} & \boldsymbol{A}_{DC\_RLC} & \boldsymbol{A}_{VSI\_RLC} & \boldsymbol{A}'_{RLC} \end{bmatrix}$$

B_{FINAL} matrix is not shown as it doesn't involve in small signal stability analysis and complexity.

Sub matrices inside the A_{FINAL} matrix are shown below.

$$\boldsymbol{A}_{G\_M} = \begin{bmatrix} 0 & 0 \\ 0 & 0 \\ 0 & 0 \\ 0 & \dfrac{3n_p\psi_{PM}}{2J_1 L_{qs}} \end{bmatrix} \quad \boldsymbol{A}_{M\_G} = \begin{bmatrix} 0 & 0 & 0 & L_{qs} i_{qs0} + \psi_{qs0} \\ 0 & 0 & 0 & \dfrac{K_{p1}K_{p2} i_{ds0} i_{qs0} L_{qs} + \psi_{PM} - L_{ds} i_{ds0}}{1 - K_{p1}K_{p2} i_{qs0}} \end{bmatrix}$$

$$\boldsymbol{A}'_G = \begin{bmatrix} -\dfrac{K_{p2}}{L_{ds}} & 0 \\ \dfrac{\omega_b L_{ds} - K_{pm}K_{p1} i_{ds0}\left(K_{p2} - R_s\right) - K_{pm}K_{p1}u_{ds0}}{\left(1 - K_{pm}K_{p1} i_{qs0}\right)L_{ds}} - \omega_b & -\dfrac{K_{pm}K_{p1} i_{ds0}\omega_b L_{qs} + K_{pm}K_{p1}u_{qs0} + K_{p1} - R_s}{\left(1 - K_{pm}K_{p1} i_{qs0}\right)L_{qs}} - \dfrac{R_s}{L_{qs}} \end{bmatrix}$$

$$\boldsymbol{A}_{GSR\_G} = \begin{bmatrix} 0 & 0 & -K_{i2} \\ \dfrac{-K_{p1}K_{im}}{1 - K_{pm}K_{p1} i_{qs0}} & \dfrac{-K_{i1}}{1 - K_{pm}K_{p1} i_{qs0}} & \dfrac{-K_{pm}K_{p1} i_{ds0} K_{i2}}{1 - K_{pm}K_{p1} i_{qs0}} \end{bmatrix}$$

$$\boldsymbol{A}_{G\_GSR} = \begin{bmatrix} 0 & 0 & 0 & -L_{qs} i_{ds0} i_{qs0} - \dfrac{\left(K_{pm}K_{p1} i_{ds0} i_{qs0} L_{qs} + \psi_{PM} - L_{ds} i_{ds0}\right) i_{qs0}}{1 - K_{pm}K_{p1} i_{qs0}} \\ 0 & 0 & 0 & K_{pm}\left[-L_{qs} i_{ds0} i_{qs0} - \dfrac{\left(K_{pm}K_{p1} i_{ds0} i_{qs0} L_{qs} + \psi_{PM} - L_{ds} i_{ds0}\right) i_{qs0}}{1 - K_{pm}K_{p1} i_{qs0}} \right] \\ 0 & 0 & 0 & 0 \end{bmatrix}$$

$$\boldsymbol{A}_{DC\_GSR} = \boldsymbol{0}_{3\times 1}$$

$$\boldsymbol{A}'_{GSR}=\begin{bmatrix}\dfrac{K_{p1}K_{im}i_{qs0}}{1-K_{pm}K_{p1}i_{qs0}} & \dfrac{K_{i1}i_{qs0}}{1-K_{pm}K_{p1}i_{qs0}} & \dfrac{K_{i2}i_{ds0}}{1-K_{pm}K_{p1}i_{qs0}}\\ \dfrac{K_{pm}K_{p1}K_{im}i_{qs0}}{1-K_{pm}K_{p1}i_{qs0}}+K_{i1} & \dfrac{K_{pm}K_{i1}i_{qs0}}{1-K_{pm}K_{p1}i_{qs0}} & \dfrac{K_{pm}K_{i2}i_{ds0}}{1-K_{pm}K_{p1}i_{qs0}}\\ 0 & 0 & 0\end{bmatrix}$$

$$\boldsymbol{A}_{M\_DC}=\begin{bmatrix}0 & 0 & 0 & -L_{qs}i_{ds0}i_{qs0}-\dfrac{\left(K_{pm}K_{p1}i_{ds0}i_{qs0}L_{qs}+\psi_{PM}-L_{sd}i_{ds0}\right)i_{qs0}}{1-K_{pm}K_{p1}i_{qs0}}\end{bmatrix}$$

$$\boldsymbol{A}_{G\_DC}=\begin{bmatrix}\dfrac{\omega_b L_{ds}i_{qs0}-\left(K_{p2}-R_s\right)i_{ds0}\left(1-2K_{pm}K_{p1}i_{qs0}\right)-2K_{pm}K_{p1}V_{ds0}i_{qs0}+V_{ds0}}{\left(1-K_{pm}K_{p1}i_{qs0}\right)L_{ds}} & \dfrac{\omega_b L_{qs}i_{ds0}+\left(K_{p1}-R_s\right)i_{qs0}+V_{qs0}}{\left(1-K_{pm}K_{p1}i_{qs0}\right)L_{qs}}\end{bmatrix}$$

$$\boldsymbol{A}_{GSR\_DC}=\begin{bmatrix}\dfrac{K_{p1}K_{im}i_{qs0}}{1-K_{pm}K_{p1}i_{qs0}} & \dfrac{K_{i1}i_{qs0}}{1-K_{pm}K_{p1}i_{qs0}} & \dfrac{K_{i2}i_{ds0}}{1-K_{pm}K_{p1}i_{qs0}}\end{bmatrix}$$

$$\boldsymbol{A}'_{DC}=\begin{bmatrix}-K_{p3}K_{p4}i_{dg0}\end{bmatrix}$$

$$\boldsymbol{A}_{VSI\_DC}=\begin{bmatrix}K_{p4}K_{i3}i_{dg0}\left(\dfrac{K_{p5}K_{p6}i_{qg0}^2}{1+K_{p5}K_{p6}V_{qg0}}+1\right) & K_{i4}i_{dg0}\left(\dfrac{K_{p5}K_{p6}i_{qg0}^2}{1+K_{p5}K_{p6}V_{qg0}}+1\right) & \dfrac{K_{p5}K_{i5}i_{qg0}}{1+K_{p5}K_{p6}V_{qg0}} & \dfrac{K_{i6}i_{qg0}}{1+K_{p5}K_{p6}V_{qg0}}\end{bmatrix}$$

$$\boldsymbol{A}_{RLC\_DC}=\begin{bmatrix}-K_{p3}i_{dg0}-\dfrac{K_{p5}K_{p6}V_{qg0}i_{qg0}}{1+K_{p5}K_{p6}V_{qg0}}+u_{dg0} & \dfrac{\left(K_{p5}V_{dg0}-1\right)K_{p6}i_{qg0}}{1+K_{p5}K_{p6}V_{qg0}}+V_{qg0} & 0 & 0\end{bmatrix}$$

$$\boldsymbol{A}_{DC\_VSI}=\begin{bmatrix}-1 & -K_{p3} & 0 & 0\end{bmatrix}^T$$

$$\boldsymbol{A}_{RLC\_VSI}=\begin{bmatrix}0 & 0 & 0 & 0\\ -1 & 0 & 0 & 0\\ -V_{qg0} & V_{dg0} & 0 & 0\\ -K_{p5}u_{qg0} & K_{p5}V_{dg0}-1 & 0 & 0\end{bmatrix}$$

$$\boldsymbol{A}_{DC\_RLC}=\begin{bmatrix}-\dfrac{K_{p3}K_{p4}\omega_b}{X_{TL}} & 0 & 0 & 0\end{bmatrix}^T$$

$$\boldsymbol{A}_{VSI\_RLC} = \begin{bmatrix} \dfrac{\omega_b K_{i3} K_{p4}}{X_{TL}} & \dfrac{\omega_b K_{i4}}{X_{TL}} & 0 & 0 \\ \dfrac{\omega_b K_{p5} K_{p6} i_{qg0} K_{i3} K_{p4}}{\left(1 + K_{p5} K_{p6} u_{Vqg0}\right) X_{TL}} & \dfrac{\omega_b K_{p5} K_{p6} i_{qg0} K_{i4}}{\left(1 + K_{p5} K_{p6} V_{qg0}\right) X_{TL}} & \dfrac{\omega_b K_{p5} K_{i5}}{\left(1 + K_{p5} K_{p6} V_{qg0}\right) X_{TL}} & \dfrac{\omega_b K_{i6}}{\left(1 + K_{p5} K_{p6} V_{qg0}\right) X_{TL}} \\ 0 & 0 & 0 & 0 \\ 0 & 0 & 0 & 0 \end{bmatrix}$$

$$\boldsymbol{A}'_{RLC} = \begin{bmatrix} \dfrac{\omega_b}{X_{TL}}\left(-R_{TL} - K_{p5} K_{p6} V_{qg0}\right) & \omega_b\left(1 + \dfrac{\left(K_{p5} V_{dg0} - 1\right) K_{p6}}{X_{TL}}\right) & -\dfrac{\omega_b}{X_{TL}} & 0 \\ -\omega_b\left(1 + \dfrac{K_{p5} K_{p6} V_{qg0}}{X_{TL}\left(1 + K_{p5} K_{p6} V_{qg0}\right)}\right) & \dfrac{\omega_b}{X_{TL}}\left(\dfrac{\left(K_{p5} V_{dg0} - 1\right) K_{p6}}{1 + K_{p5} K_{p6} V_{qg0}} - R_{TL}\right) & 0 & \dfrac{-\omega_b}{X_{TL}} \\ -\omega_b X_C & 0 & 0 & \omega_b \\ 0 & -\omega_b X_C & -\omega_b & 0 \end{bmatrix}$$

$\mathbf{A_M}$ and $\mathbf{A_{VSI}}$ are same as described in developing models.